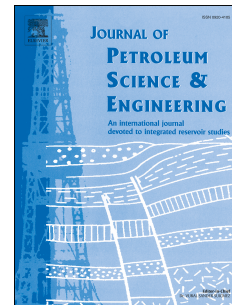


Accepted Manuscript

Fluid mechanics of hydraulic fracturing: A review

Andrei A. Osiptsov



PII: S0920-4105(17)30492-8

DOI: [10.1016/j.petrol.2017.05.019](https://doi.org/10.1016/j.petrol.2017.05.019)

Reference: PETROL 4003

To appear in: *Journal of Petroleum Science and Engineering*

Received Date: 7 March 2017

Revised Date: 16 May 2017

Accepted Date: 18 May 2017

Please cite this article as: Osiptsov, A.A., Fluid mechanics of hydraulic fracturing: A review, *Journal of Petroleum Science and Engineering* (2017), doi: 10.1016/j.petrol.2017.05.019.

This is a PDF file of an unedited manuscript that has been accepted for publication. As a service to our customers we are providing this early version of the manuscript. The manuscript will undergo copyediting, typesetting, and review of the resulting proof before it is published in its final form. Please note that during the production process errors may be discovered which could affect the content, and all legal disclaimers that apply to the journal pertain.

Fluid mechanics of hydraulic fracturing: a review

Andrei A. Osiptsov^a

^a*Skolkovo Institute of Science and Technology (Skoltech), 3 Nobel Street, 143026, Moscow, Russian Federation*

Abstract

Although hydraulic fracturing is a mature technology that has been used commercially since the late 1940s, the development of unconventional hydrocarbon fields with the combination of directional drilling and multistage hydraulic fracturing in the last two decades gave rise to a substantial progress in both operations and associated modeling. Numerical simulators, based on those models, are key to the design and evaluation of hydraulic fracturing treatments. Though hydraulic fracturing is a truly coupled phenomenon, the solid mechanics part of the problem has typically received more attention than the fluid mechanics part. Yet, that fluid mechanics field is a very rich multidisciplinary domain, presenting a number of challenges posed by the contemporary technology advancement, most of which being still unresolved. This paper aims to review the state of the art in multiphase fluid mechanics modeling of hydraulic fracturing, highlighting gaps in the body of knowledge and clarifying the questions that are still open.

This review sheds light on critical phenomena peculiar to hydraulic fracturing treatments, which are grouped into three categories (according to subsequent stages of the stimulation treatment): (i) proppant transport down the wellbore, (ii) proppant placement into the fracture, (iii) flowback from fractures into a well after the end of stimulation treatment (which is particularly important for preserving the integrity and conductivity of the fracture network). To support the modeling in these areas, constitutive relationships calibrated by experiments are of paramount importance. The list of phenomena, still not fully covered by modeling, includes: slugs dispersion in the well during alternate-slug fracturing, impact of fibers and visco-elasto-plasticity of the fracturing fluid on proppant placement in fractures, effects of complex rock fabric and real fracture morphology (roughness, steps, ledges, turns, and junctions), transition from dense suspension to close packing, dynamic bridging and mobilization, particle sedimentation to form a packed bed and re-suspension, dune transport in fracture network, overflush, and flowback into the near-horizontal well from fractures, to name a few. All these effects need to be properly accounted for in the hydraulic fracturing simulators in order for the contemporary technology of multistage fracturing to be designed, executed, evaluated, and optimized properly and safely to yield optimum production, especially in unconventional reservoirs.

Keywords: multiphase flow, flowback, hydraulic fracturing, proppant transport, shales, suspension, bridging, leakoff, well, particle, fracture, multistage fracturing, overflush, well, packing, granular rheology

1. Introduction

Hydraulic fracture propagation is a coupled problem of solid mechanics (fracture opening and growth) and multiphase fluid mechanics (slurry transport down the wellbore and placement in the fracture). The geomechanics aspect of hydraulic fracturing is thoroughly reviewed (see [18], and the most recent [49]). Whereas, the main aim of this paper is to critically review the fluid mechanics aspects of the process. We will look at the models of multiphase flows in wells and fractures, which are used in hydraulic fracture simulators, and highlight the gap between the state of the art in the development of technology and that in modeling. The latter typically advances with a certain lag behind the technology. In simulations of hydraulic fracturing, the focus is usually made on geomechanics of hydraulic fracture propagation, while fluid mechanics is deprioritized and simplistic models are used to track proppant during transport down the wellbore and placement inside the fracture.

At the same time, new technologies rolled out to the market recently, to develop both conventional and unconventional (source rocks) reservoirs utilizing complex fluid systems with solids admixtures, which are placed to keep fractures open and provide a conductive path for hydrocarbons from far field to the wellbore. The rheology of the carrier fluid is non-Newtonian and often can be characterized as visco-elasto-plastic due to added polymers [20]. The shear thinning nature of the carrier fluid helps reduce hydraulic resistance while pumping the slurry down the wellbore. On the other hand, the mixture develops a yield-stress behavior. Yield stress of the mixture can be both due to cross-linking of the polymer gel or due to the presence of the fibers. Cross-linking of the gel due to delayed chemical reactions, right about before the mixture enters the fracture through perforations, is designed on purpose to prevent undesired settling of solids to the bottom of the fracture. Fibers [69] are used as one of the key agents to keep the proppant-fluid mixture coherent and prevent proppant settling as well as creating fracture width. Fiber-laden fracturing fluids have been used routinely in the field for more than a decade now [59], and yet

Email address: a.osiptsov@skoltech.ru (Andrei A. Osiptsov)

the impact of fibers on rheology and settling is not taken fully into account in fracturing simulators. Alternate-slug pumping for channel fracturing is now commonly used [76, 143] as a technique to provide channels supported by proppant pillars in the fracture, but proper modeling of slug dispersion, while transported down the wellbore and through perforations, still awaits systematic theoretical attention (not to speak about slugs interaction with rough fracture surfaces). Finally, in-situ channelization of fiber-proppant slurry in a closing fracture has been recently introduced [163, 121], but again the technique of channelization is rather based on lab experiments in slots and field testing, than on modeling.

There is a clear need for multi-scale sub-models and associated development of the global modeling framework to integrate these sub-models properly. The relevant phenomena exhibit a hierarchy of length scales, which we briefly list below in increasing order of scale:

- At the scale of the proppant grain: interaction between particles and fibers and proppant-fiber net building, lateral motion of a particle, settling, saltation;
- Perforation diameter: proppant slug break down and dispersion, gel breaking and re-cross-linking, shear recovery;
- Fracture width: fibers contact with fracture walls and effect on proppant settling, shear-induced and inertial migration of proppant, non-uniform proppant concentration profile;
- Well diameter: proppant settling in horizontal wells, effects on proppant slug dispersion;
- Fracture length/height: proppant placement and settling, proppant bed formation, resuspension, proppant transport in a fracture network, shear banding, dune transport;
- Well length: proppant slug transport and dispersion;

Our mental picture of the necessary mission in fluid mechanics of hydraulic fracturing is as follows: construct a hierarchy of models according to the hierarchy of scales; define the links between models developed on different scales (upscaling), where the models developed on smaller scales typically enter into the larger-scale global modeling framework as a constitutive relationship (closure relation); develop a consistent experimental program to calibrate small-scale models and validate the entire large-scale modeling workflow; and finally, the modeling workflow should be tested against real fracturing jobs in the field. The key fundamentals of the technology of hydraulic fracturing and related terminology can be found in [57].

The focus of the paper is on *transport phenomena* associated with multiphase flows during hydraulic fracturing treatment and at the stage of cleanup and flowback from a fractured well. We will cover the fundamental issues of fluid mechanics in hydraulic fracturing of wells drilled in both conventional and unconventional reservoirs. Conventional fracturing is characterized by typically using cross-linked polymer gels as a treatment fluid with high proppant loading (volume fraction of 0.3–0.4). Cross-linked fracturing fluids are exhibiting shear-thinning behavior and yield stress, both adequately described by the Herschel-Bulkley rheology model, and visco-elastic effects typically dismissed by the fracturing simulators. Whereas, high-rate slick-water fracturing in shales is usually done with shear-thinning fluids (dilute aqueous solution of polymer-based

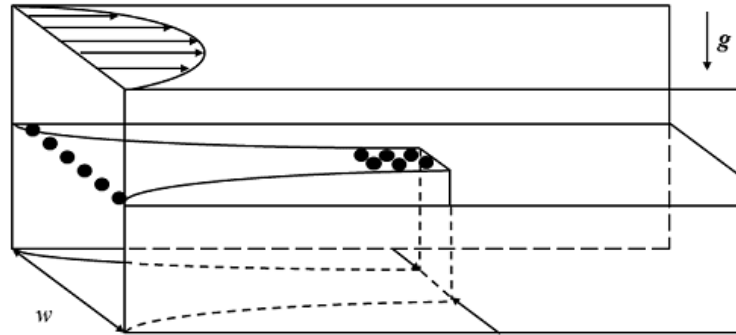


Figure 1: Sketch of suspension transport in a vertical fracture.

drag reducers) and particles at small volume fraction, below 0.1 [57, 18, 20]. There is, however, more and more of a tendency to end the treatment with conventional-like slurries (so-called hybrid operations). Furthermore, alternate slug-pumping with the addition of fibers to the slurry is now routinely carried out in both conventional and unconventional reservoirs. Thus, the present paper will keep as much as possible a uniform focus throughout the range of fracturing applications to various types of reservoirs.

We split the entire body of research on fluid mechanics of hydraulic fracturing into three major groups in terms of geometry and flow regime: creeping viscosity-dominated 2D flows in fractures (reviewed in Sec. 2) and high-Re inertia-dominated 1D flows in wells (Sec. 3) during pumping a fracturing job, and, separately, multiphase flows during flowback from a multistage fractured wells (Sec. 4). Properly selected constitutive relationships (Sec. 5) are of universal importance for closure of the models, to make them self-contained and predictive. The review ends up with conclusions (Sec. 6).

2. Suspension placement in fractures

Accurate prediction of proppant placement into hydraulic fractures is one of the key requirements to design and planning of successful hydraulic fracturing jobs. Barring cases based solely on return on experience, the design is formulated using a model-based hydraulic fracturing simulator. Success here implies the fracturing treatment is executed in the field in the same way as it was planned ahead using the hydraulic fracturing simulator, which means the model underlying the simulator should provide a close rendition to reality. Otherwise, there may be unexpected events during pumping when models do not capture some important effects in geomechanics (uncontrolled fracture height growth resulting in fracture breakthrough into upper or lower layers, premature tip screenout) or fluid mechanics (screenout on perforations due to issues with rheology, undesired settling of solids in the near-wellbore zone). There is a number of commercial simulators of hydraulic fracturing allowing to model proppant transport in open hydraulic fractures. They use different proppant transport models, both in terms of fracture flow configuration and the physical phenomena they capture.

Most commercial simulators of hydraulic fracturing available from service companies use proppant transport models based

Parameter	Units	Range of values
Fracture geometry		
Half-length	m	100 – 300
Height	m	20 – 50
Width	mm	1 – 10
Fluid properties		
Power law index, n	non-dim	0.5 – 1
Fluid consistency, K	$\text{Pa} \cdot \text{s}^n$	10^{-3} – 2
Yield stress	Pa	0 – 15
Molecular diffusivity, λ	m^2/s	10^{-9}
Relaxation time, t_r	s	5
Solids properties		
Particle diameter	m	10^{-4} – $2 \cdot 10^{-3}$
Particle substance density	kg/m^3	$2.65 \cdot 10^3$
Particle concentration	non-dim	0 – 0.4
Injection flow conditions		
Flow rate at surface, Q	m^3/min	0.6 – 6
Flow rate at surface, Q	bbl/min	4 – 40
Linear velocity, U	m/s	0.2 – 20

Table 1: Range of dimensional parameters typical for hydraulic fracturing operations.

on simplified 1D approaches to fluid mechanics developed to provide robust integration into the entire numerical algorithm covering a wide range of hydraulic fracturing-related processes. These models are inherited in the simulation kernels developed in the 1980s, when the simulators of the first generation used simplistic lumped-parameter models based on mass conservation considerations. Simplifications were made due to limited computational capabilities (e.g., [70, 71, 21]).

In the 1990s, with the development of computers and numerical methods, Pseudo-3D models of fracture growth coupled with a 1D model of proppant transport were implemented in simulators (e.g., [168, 135]). Such proppant transport models were later extended in 2D for illustration of placement, while the height-averaged 1D model was still used for coupling with the geomechanics module [190]. In the early 2000s, the assumptions behind the Pseudo-3D approximation were relaxed in the development of Planar-3D models, where the fracture could have an arbitrary yet planar shape, which allows for a fully 2D model of proppant transport accounting for settling and slumping, bed formation, packing, bridging and tip screen-out.

Finally, the late 2000s saw a massive development of multi-stage fracturing technology for stimulation of near-horizontal wells in unconventional reservoirs, which called for simulators of complex fracture networks. Examples include: the Unconventional Fracture Model (UFM) [209], which describes the growth of fracture network in a porous medium with pre-defined naturally faults (oriented arbitrarily and not necessarily connected), the Wiremesh model [218], which is designed for fracture net growth on a pre-defined regular network of connected natural fractures; DFN models implemented in extensions of the model first presented in [119, 120], which simulate multiple, cluster, and discrete type fractures in shales and CBM

based on the discrete fracture network approach.

In addition to the major effort by service companies to develop fracturing simulators for design and execution control of the fracturing technology, in the 2010s some national oil companies started developing their proprietary fracturing software with complex functionality as well (e.g., P3D and Planar-3D models with 2D proppant transport [5]) to have an internal benchmark solution.

There is also a family of emerging research simulators from academia and corporate research centers, which are based on more advanced 2D approaches allowing to focus on accurate modeling of proppant placement. The following list is by no means complete and is given here to show the variability: coupled simulators UTFRAC-3D by University of Texas at Austin [180], Spatially Heterogenous Aperture Code (SHAC) [126, 127] (covering the flow of Herschel-Bulkley fluid in a variable-aperture fracture), CFRAC simulator [188, 189] (allows for simultaneous modeling of fracture propagation and closure, and proppant transport, also in discrete fracture networks), and the simulator for the growth of fracture network in shales based on the model of intersection of a primary hydraulic fracture with a pre-existing fault [25, 26]. Standalone proppant transport simulator FracFlow, based on a novel two-fluid model of suspension flow and providing proppant placement patterns for a given fracture geometry, is described in [28, 29, 31, 153, 155]. A direct numerical simulation of proppant transport using a coupled CFD-FEM approach can be found in [220, 221]. Integrated simulators of multiphase flows in the wellbore, fracture, and reservoir are also underway [201, 124].

The key assumptions and governing equations of a typical proppant transport model are summarized below. The flow is modeled within a 1D hydraulics approach or 2D lubrication approximation (a.k.a. long-wave approximation or thin-layer approximation) to 3D Navier-Stokes equations in a single vertical hydraulic fracture or a fracture network (currently only with simplified quasi-1D placement models, which at best take into account a three layer structure in the vertical direction: clean fluid, suspension and a bank at the bottom [209]). The fracture is approximated by a rectangular narrow channel of variable aperture (both in space and time), with permeable fracture walls (leak-off). Averaging over the fracture width is carried out under the assumption that cross-fracture proppant concentration profile is uniform (no migration). Carrier fluids typically have power-law rheology, but note that there may be different carrier fluids in a pumping schedule. Visco-elasticity and yield stress are neglected. As for suspended particles, the model covers settling, granular packing/jamming, several proppant types, bridging. Slumping due to gravity is covered only by 2D models (e.g., [191, 80]). Dynamics of fracture closure after the end of injection with effects of plasticity and proppant embedment is now available only in research codes (e.g., [127]).

Note that the suspension transport models mentioned above are all based on the so-called effective medium approximation following [2] and [160], where suspension is treated as a viscous incompressible fluid with viscosity and density dependent on proppant volume concentration and characterized

No.	Parameter	Expression	Range of values
1	$Bu = Re/Fr^2$	$\rho_0^0 gw/\mu_0^0 \dot{\gamma}_0$	$10^{-3} - 10^4$
2	Bn	$\tau_{p,0}/\mu_0 \dot{\gamma}_0$	$0 - 100$
3	ζ_i	ρ_i/ρ_0	$0.5 - 1$
4	M_i	μ_i/μ_0	$10^{-3} - 1$
5	τ_i	τ_i/τ_0	$1 - 10$
6	ε	w/L	$10^{-6} - 10^{-4}$
7	R	L/H	$1 - 10$
8	Re	$\rho_0 UL/\mu_0$	$1 - 10^4$
9	Re_p	$\rho_0 v_s a/\mu_0$	$1 - 10^2$
10	St/Fr^2	$mg/6\pi a\mu_0$	$10^{-8} - 10^{-2}$
11	De	t_r/t_s	$0 - 2$
12	We	$t_r \dot{\gamma}$	$0 - 10$

Table 2: Ranges of non-dimensional parameters typical for hydraulic fracturing, based on dimensional values shown in Table 1.

in terms of the volume-averaged velocity. It was convenient, as volume-averaged velocity is non-divergent (hence "incompressible" medium), but it coincides with the mass-averaged velocity only in the case of neutrally-buoyant particles frozen in the fluid. The formulation of the lubrication model of proppant transport was revisited in [28], where the model was derived from conservation laws within the two-fluid approach for suspension.

A typical proppant transport model converges to the Poisson-type elliptic equation for pressure [57, 85]:

$$\frac{\partial w}{\partial t} = \nabla \cdot \left[\frac{w^3}{12\mu} (\nabla p - \rho g) \right] + Q - \frac{2C_L}{\sqrt{t-t_0}}$$

Here the coefficient $w^2/12$ is often referred to as the hydraulic conductivity of a open hydraulic fracture (and $w^2/12\mu$ is mobility or fluidity [129]), and t_0 is the time when fluid reaches the point. A Dirichlet-type boundary value problem is set up for the pressure equation, using the boundary conditions: a given inlet velocity on perforations, no-flow conditions on top and bottom, and a "soft" non-reflecting outflow condition at the outlet (if a near-wellbore fracture area only is considered). Based on the pressure field, the velocity is calculated via the Darcy-like expression via the pressure gradient, and proppant concentration is obtained from solving the advection equations. Typical dimensional parameters for the flow inside a hydraulic fracture are shown in Table 1. The list of typical values of non-dimensional parameters is shown in Table 2.

Here, the Deborah number $De = t_r/t_s$ is the ratio of the characteristic relaxation time of the medium t_r to the characteristic time of the deformation process t_s , the Weissenberg number $We = t_r \dot{\gamma}$ is the product of the relaxation time t_r and the mean shear rate $\dot{\gamma}$, where the mean shear rate is given by: $\dot{\gamma} = U/w$.

2.1. Two-fluid model of suspension flow in fractures

Now let us elaborate on the difference between the effective-fluid approximation and the two-fluid approach. We present below the two-continua model of proppant transport derived from conservation laws in the two-speed approximation, where particles and carrier fluid are treated as two interpenetrating and

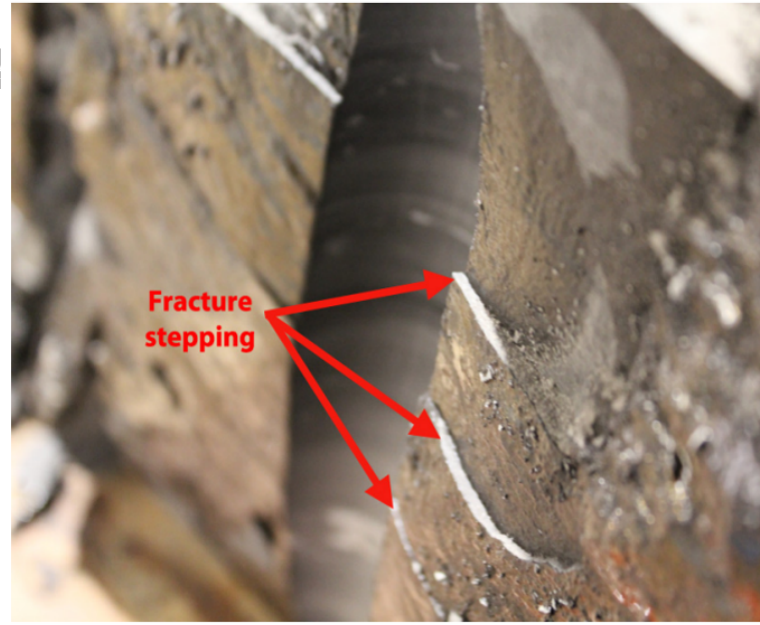


Figure 2: Photograph of the face of a hydraulic fracture created in the laboratory. Steps are highlighted.

interacting continua [28]:

$$\frac{\partial w C_p}{\partial t} + \nabla (w C_p \mathbf{v}_p) = 0 \quad (1)$$

$$= \nabla \left[\frac{w^3}{12\mu(C)} (\nabla p + Bu [1 + C_p(\zeta_p - 1)] \mathbf{e}_2) - w C_p \mathbf{v}_s \right] \quad (2)$$

$$\mathbf{v}_f = -\frac{w^2}{12\mu(C_p)} (\nabla p + Bu [1 + C_p(\zeta_p - 1)] \mathbf{e}_2) \quad (3)$$

$$\mathbf{v}_p = \mathbf{v}_f + \mathbf{v}_s, \quad \mathbf{v}_s = -\frac{St}{\zeta_p Fr^2} (\zeta_p - 1) f(C_p) \mathbf{e}_2 \quad (4)$$

$$f(C_p) = \left(1 - \frac{C_p}{C_{max}} \right)^{\alpha} \quad (5)$$

This model differs from the earlier effective-fluid models [160] by an extra term $-w C_p \mathbf{v}_s$ due to two-speed effects in the pressure equation. It was shown [28] that this term is important at low Bu (e.g., for low-viscosity fluids) and leads to up to 20% difference in the estimated area of a propped fracture in slick water treatments, while for conventional fracturing the two models basically match. At the same time, the question as to which model, the effective-fluid or the two-continua, is closer to the lab data is still unresolved and awaits consideration within a properly designed experimental program on slot tests.

Equations for the displacement of fracturing fluids in a fracture taking a yield stress into account were derived in [31], which can be used as an extension to the models of proppant transport by explicitly including the yield stress in the following way:

$$\begin{aligned} \frac{\partial w(1 - C_p) C_i}{\partial t} + \operatorname{div}(w(1 - C_p) C_i \mathbf{v}_f) = \\ -2(1 - C_p) C_i v_l \end{aligned} \quad (6)$$

$$\frac{\partial wC_p}{\partial t} + \operatorname{div}(wC_p \mathbf{v}_p) = 0 \quad (7)$$

$$\operatorname{div}\left(\frac{w^3}{12\mu_m} [\Phi(\vartheta)\nabla p + Bu\rho_m \mathbf{e}_2] - wC_p \mathbf{v}_s\right) = -\frac{\partial w}{\partial t} - 2(1 - C_p)v_l, \quad (8)$$

$$\rho_m = 1 + C_p \left(\zeta_p - \sum_{i=1}^{i=n} \zeta_i C_i \right)$$

$$\mathbf{v}_f = -\frac{w^2}{12\mu_m} \Phi(\vartheta) \nabla p, \quad (9)$$

$$\mathbf{v}_s = -\frac{Stf(C_p)\Phi(\vartheta)}{\zeta_p Fr^2} \left(\zeta_p - \sum_{i=1}^{i=n} \zeta_i C_i \right) \mathbf{e}_2, \quad (10)$$

$$\Phi(\vartheta) = 1 - 3\vartheta + 4\vartheta^3, \quad \vartheta = \frac{Bn\tau_m}{w|\nabla p|} \quad (11)$$

Note that in (1)–(3) and (6–11) differential operators ‘div’ and ‘ ∇ ’ act in the (x, y) plane as we applied averaging procedure over the z -direction. The system of averaged governing equations involves hyperbolic transport equations for concentrations of fluids and particles (6), (7) and a quasi-linear elliptic equation for pressure (8). In the case of Newtonian fluid flow in a slot ($\Phi(\vartheta) = 1$) there is a well-known analogy with the flow in a porous medium (Darcy law for fluid velocity) [174]. Expression for the width-averaged particle settling velocity (9) involves the relative width of the yielding zones at the current location along the slot, which is equal to $\Phi(\vartheta)$.

As outlined above, there are different formulations of proppant transport models (a family of effective fluid models and the two-fluid model), hence there is a need for validation against lab data to evaluate the accuracy and applicability of the models. Especially, validation is required that is relevant at the scale of hydraulic fracturing treatment. At the same time, it has been quite widely accepted in the relevant literature that it is practically impossible to ensure a dynamic similarity between a lab experiment on proppant transport and a fracturing operation in the field (e.g., this issue is discussed in [203]). This conclusion can be quickly made from the dimensional analysis based on Table 2. It is, however, possible to consider a certain subset of nondimensional parameters and focus on a particular phenomenon governed by these groups, so that the similarity between the lab and the field is possible. For example, the validation was carried out in [31] against a set of lab tests on slumping (Bu, ζ_i), and a separate a set of tests on fingering in Newtonian and Bingham fluids (Bn, M_i).

The existing models of proppant transport implemented into hydraulic fracturing simulators can be improved in at least two ways: by adding more relevant physics, and by improving the numerical performance of the simulators on fine meshes to capture small-scale phenomena. Key phenomena missing, or to be significantly improved, in existing models are: particle transport by dune movement in high-rate water fractures; effects of foaming fracturing fluids when put in contact with hydrocarbons, which should improve their flowback and cleanup efficiency; effects of temperature, visco-elasticity and fibers on

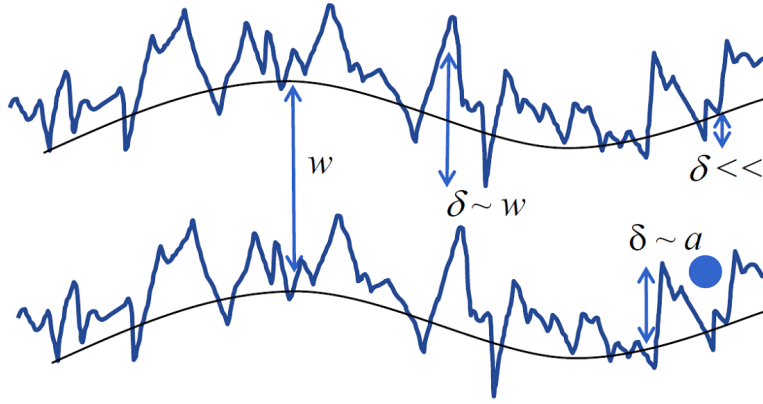


Figure 3: Scheme of the real fracture morphology: w – real fracture opening (distance between points on opposite fracture faces), d – fracture aperture (averaged characteristic), δ – scale of roughness.

density and rheology of the suspensions. On the numerical side, the simulators need improved linear and non-linear pressure solvers based on up-to-date numerical methods (e.g., variants of multigrid algorithms [33, 31]), ability to resolve very small proppant pillars to model heterogeneous proppant placement during alternate-slug fracturing (with large meshes); improved advection schemes: fast and accurate resolution of interfaces. In what follows, we will discuss these aspects in a more detail.

2.2. Impact of real fracture morphology

All existing models of proppant transport are constructed in the so-called lubrication approximation, which assumes that the fracture is a plane channel with the width being a smoothly varying function of spatial coordinates: $\nabla w(x, y) \ll 1$. Real fractures, especially in shales, are breaking this assumption (see Fig. 2). Effect of non-planar fracture geometry manifests itself in the following (see Fig. 3 for illustration):

– “The 300ft problem” – from the mental picture of a stimulated network based on big block experiments and production field data of multistage fractured wells in shales, it follows that the fracture network connectivity is lost beyond an average of 200–400 ft from the well [199]. A study on large shale outcrops revealed that the entire fracture system can be classified into three zones: (i) the connector between the wellbore and the fracture system (20–30 ft), (ii) the near-wellbore fracture (200–400 ft) and (iii) the far-wellbore fracture network. Zone (iii) can become hydraulically disconnected from the wellbore for the following reasons: poor proppant delivery due to multiple turns, junctions and crossings with weak interfaces, where particles bridge and stop; and even if zone (iii) is propped during placement, the conductivity can be lost during flowback and well start-up due to dynamic interplay between proppant movement (fracture closure and pinch-out) and fines migration (permeability damage of the proppant pack). Current proppant transport models are adequate but for this problem, and below we elaborate on various elements contributing to this issue.

– wall roughness (of the length scale δ), which could be included into the lubrication model as an additional drag exerted on the flowing suspension from the fracture surfaces;

– sharp discontinuities on the fracture surfaces, e.g., stepovers, ledges, (see Fig. 2), which may be treated as extra bound-

ary conditions imposed on a certain line (e.g., no-flow for proppant on a line which marks a near-horizontal step or ledge); note that, these can trigger discontinuous phenomena on proppant transport – such as accumulation, jamming, bridging, arching, etc.

- fracture turns/intersections with natural fractures and re-initiation from those natural fractures, leading to jogs in the flow path;

- sudden fracture constriction or expansion at the point of intersection with a pre-existing fault or a natural fracture, which can be treated as a point loss of momentum (similar to a choke in hydraulics);

- more generally, transport in a developed fracture network, with motion round the corners/junctions, also including dune transport [117] and saltation/resuspension in networks; in slick water fractures in shales, one of the hypotheses is that proppant almost fully settles in the primary fracture and then translates by dune movement [117, 136];

- pinch-out points and lines, which result in the local loss of proppant mobility, yet the fracture remains permeable for fluid;

- effect on slurry slug dispersion due to interactions with rough walls;

- "wedge fracturing" – the concept closely related to overflushing, where the upper area of the fracture is unproped but remain open by the wedging action of proppant trapped in the closed fracture below [117].

Various elements of the real fracture morphology can be classified in terms of their relative length scale and impact on transport. The illustration of the hierarchy in the form of a graph is given in Fig. 4.

In the case of natural fractures, which are mostly due to shear, in contrast to hydraulic fractures, which are tensile cracks, there are theoretical studies of the effect of surface roughness on fluid flow through rock joints (e.g., [36]). Deviations from the lubrication model are expected because real joint surfaces are rough and contact each other at discrete points. Realistic rough surfaces were generated numerically using a fractal model of surface topography. Numerical simulations were performed for various surface roughnesses (fractal dimensions), and the hydraulic aperture was compared to the mean separation of the surfaces. It was shown [36] that for large apertures, the surface topography has little effect. At small separations the flow is tortuous, tending to be channeled through high-aperture regions. The parameter most affecting fluid flow through rough joints is the ratio of the mean separation between the surfaces to the root-mean-square surface height (while variations in the fractal dimension have only a slight effect [36]). There is also a chain of theoretical papers on correlations for the aperture of a fractal fracture, where the opening is due to shear of two mirror-image fractal surfaces [215].

We may propose a working hypothesis here that the impact of real fracture morphology on fluid flow inside a hydraulic fracture may be taken into account along the same lines as it was done in the theory of natural fractures and fractal joints. This hypothesis needs to be thoroughly researched though, before judging on its applicability. As for the real morphology of *hydraulic* fractures, there are much fewer papers (as compared

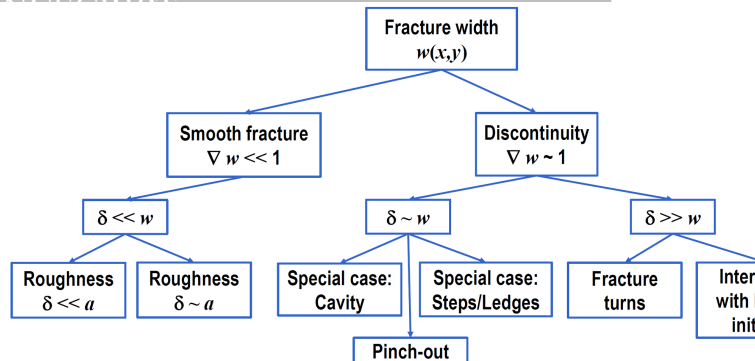


Figure 4: Hierarchy of length scales of real fracture morphology and its impact on proppant transport: fracture width $w(x,y)$, morphology element of the size δ , and proppant radius a .

to natural fractures discussed above), but we would mention the work [210], which specifically studied the roughness of hydraulic fracture surfaces viewed as a result of the processes in the zone ahead of the tip. It was shown that the fracture surface roughness correlates with a measure of the plastic zone size around the fracture tip.

Fracture network. Another phenomenon, which is important to describe in view of generalization of existing proppant transport models for fractured unconventional reservoirs, is proppant transport in fracture network: effects of complex geometry (stepovers, corners, junctions, pinch-points, see Figs. 2–4) on placement need to be precised and included. There is ongoing effort on modeling dense suspension flows in branching networks, e.g. see [184]. Experimental study of proppant transport in complex fracture network is carried out in [185]. It was argued that, while transported in secondary fractures closer to the wellbore, the proppant is expected to be "turning round the corner" if the flow velocity is higher than some threshold value [20]. Currently, all existing proppant placement simulators dealing with fracture networks are essentially 1D and missing various critical 2D phenomena. The approaches to model solids transport in complex fractures could be based on the Lagrangian modeling and improvements of existing lubrication models, explicitly taking into account the elements of complex fracture morphology in two ways: (i) as boundary conditions on lines within 2D flow domain (no-flow condition for proppant on steps, ledges, and junctions), or (ii) as distributed extra drag on slurry (effect of surface roughness on proppant retardation and hindered settling).

2.3. Particle migration

Proppant transport models in commercial simulators of hydraulic fracturing (and in most of the research codes) are all based on the assumption of a uniform cross-fracture concentration profile, which makes it possible to integrate 3D reduced asymptotic equations over the width and come up with a 2D averaged system of equations. At the same time, there is evidence that particles do migrate in pressure-driven suspension flows in channels from the walls towards the channel middle plane (see, e.g., experiments in [203]), which results in higher rates of particle transport along the fracture and higher rates of sedimentation [206, 29]. The physical phenomena contributing

		Dilute suspension
Newtonian	No-slip	Neutrally-buoyant particles in Poiseuille pipe flow Segre&Silbergberg 1962, experiment $R_{eq} = 0.62R$ [178] $\mathbf{F}_L = \pi a^3 \rho_f [\mathbf{V}_p \times \Omega_p]$ (Rubinow&Keller, 1961 [173]) $\mathbf{F}_L = \rho_f U^2 a^4 c_L(r/R), \text{Re}_c \rightarrow 0, R_{eq} = 0.6R$ (Ho-Leal, 1974 [88], Vasseur-Cox, 1976 [212]) $\text{Re}_c < 100 : \mathbf{F}_L = \rho_f \dot{\gamma}^2 a^4 c_L^{SH}$ (Schonberg-Hinch, 1989 [95]) Plane channel: $100 < \text{Re}_c < 3000 : \mathbf{F}_L = \rho_f \dot{\gamma}^2 a^4 c_L(r/l, \text{Re}_c)$ (Asmolov, 1999 [7]) Circular pipe: $1 < \text{Re}_c < 2000 : \mathbf{F}_L \sim \rho_f \dot{\gamma}^2 a^4 c_L$ (Matas, Morris, Guazzelli, 2009 [116])
		Linear fluid velocity profile Slip in plane $\mathbf{v}_s \in (\mathbf{v}_f, \dot{\gamma})$ (Fig. 5a): Strong shear: $\mathbf{F}_L = 6.46 \mu_f a^2 v_s (\dot{\gamma}/\nu)^{1/2}$ (Saffman, 1965 [175]) Arbitrary shear: $\mathbf{F}_L = \mu_f a^2 v_s (\dot{\gamma}/\nu)^{1/2} c_L (\text{Re}_p/\text{Re}_G^{1/2})$ (Asmolov, 1990 [8], McLaughlin, 1991 [122])
		Quadratic fluid velocity profile Slip in plane $\mathbf{v}_s \in (\mathbf{v}_f, \dot{\gamma})$ (Fig. 5a): $\mathbf{F}_L \sim \mu_f a^2 v_s (\dot{\gamma}/\nu)^{1/2}$ (Asmolov, 1999 [7])
		Slip in plane $\mathbf{v}_s \in (\mathbf{v}_f, \dot{\gamma})$ (Fig. 5a): $\mathbf{F}_L = \mu_f a^2 v_s (\dot{\gamma}/\nu)^{1/2} c_L (\text{Re}_p/\text{Re}_G^{1/2}, d/L_{Sa})$ (Asmolov, 1990 [8], McLaughlin, 1991-93 [122, 123])
		Slip in plane $\mathbf{v}_s \in (\mathbf{v}_f, \dot{\gamma})$ (Fig. 5a): $\mathbf{F}_L = \pi V \left[\frac{9}{16} \nu + \frac{3}{16} \frac{d}{l_p} (22 - 105 \frac{d}{l_p} \text{Re}_c^{1/2}) \right]$ $\text{Re}_c \rightarrow 0 : (\text{Cox}&\text{ Hsu}, 1977 [45])$ $\mathbf{F}_L \sim \mu_f a^2 v_s (\dot{\gamma}/\nu)^{1/2}$ $\text{Re}_c < 100 : (\text{Hogg}, 1994 [90])$ $\text{Re}_c > 100 : (\text{Asmolov}, 1999 [7])$
	Slip	Slip normal to plane $\mathbf{v}_s \perp (\mathbf{v}_f, \dot{\gamma})$ (Fig. 5b): $\mathbf{F}_L = 6\pi \rho_f V_s^2 a^2 c_L (d/l, V_s, \text{Re}_c)$ (Asmolov&Osipsov, 2008 [147])
		Visco-elastic
		$F_L = -\frac{5}{3} \pi \beta \gamma (N_l - 2N_2)$ (Ho& Leal, 1976 [89]) $v_L \sim \frac{a^2}{6\pi\mu} \frac{\partial N_1}{\partial \dot{\gamma}} \frac{\partial \dot{\gamma}}{\partial y}$ (Tehrani, 1996 [203])
		Visco-elastic
		Visco-elastic

Table 3: Overview of various mechanisms contributing to a lift force exerted on a single particle in a shear flow of viscous fluid.

into the migration mechanism are quite complex, including linear and quadratic shear flow, particle slip relative to the fluid, wall effects, and effects of non-Newtonian rheology (especially normal stress difference in the case of visco-elastic fluids). Below we will consider the phenomenon of particle migration in detail in two fundamentally different cases of dilute and concentrated suspension.

Migration of single particles in dilute suspension. In dilute suspensions (typical of slick-water fracturing at small proppant loading in shales), the migration of particles in the suspension is mainly due to single-particle effects in a specified flow field. Four physical effects should be distinguished: (i) particle buoyancy (usually negative and leading to settling); (ii) particle inertia (leading to the slip of particles relative to the carrier fluid, which is typical in the entry development region where Poiseuille profile is being established); (iii) particle-wall interactions; and (iv) small but nonzero inertia of the carrier fluid.

Even in a simply formulated case of a single particle in viscous shear flow through a channel, the migration phenomenon is quite complex and sometimes causes confusion in oilfield literature, so we think it is worth spending some of the reader's time to clarify it. In Tab. 3, we present the results for the lift force acting on a single particle for various configurations, defined as $\mathbf{F}_L = 6\pi\mu u v_L$, where v_L is the lateral migration velocity. Basically the lift force is the Stokes drag force exerted on a particle due to the formation of a lateral component of the fluid flow due to the disturbance of the velocity field of the carrier fluid by the presence of the particle, which generally rotates in a shear flow and sometimes moves relative to the carrier fluid.

Fundamentally, there can be two different cases of motion of particles in a Poiseuille flow through a plane vertical channel: (i) a neutrally-buoyant particle moving with no slip relative to the main flow but subject to rotation because of the shear flow and velocity gradient even on the scale of the particle diameter;

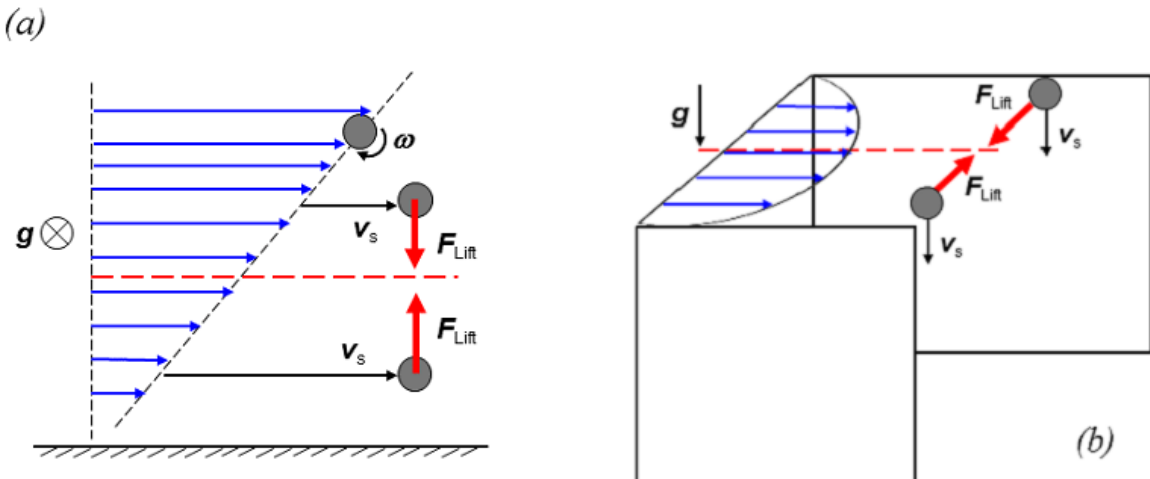


Figure 5: Lift forces on a particle when slip is in the plane [175, 147] (a), or normal to the plane [9] (b), of fluid velocity and its gradient. Neutrally-buoyant particle rotating in shear flow is also shown [178, 95] (a). Red dashed line shows particle equilibrium position, and black dashed line a) shows channel middle plane. Fluid velocity is represented by blue arrows, particle slip velocity v_s – by black arrows, and the lift force \mathbf{F}_L – by red arrows, and ω is the rotation velocity. During suspension transport in the fracture, particles first migrate in the horizontal section towards the two vertical equilibrium planes away from walls in the short entry region, where the Poiseuille velocity profile is being established (a), and then on the scale of the fracture length particles migrate towards the fracture middle plane under the lift force due to the vertical settling velocity (b).

and (ii) a non-neutrally-buoyant heavy particle moving with a certain slip velocity relative to the fluid. The case (ii) is especially relevant to proppant transport, where the entire fracture length can be split into two regions. First is a relatively short entry region, where Poiseuille velocity profile is being established (on the scale of 10 cm - 1 m) and particles are lagging behind/moving faster than the fluid in the horizontal plane of fluid velocity and its gradient. The second region is the entire fracture length, where velocity relaxation is complete, particles are "frozen" into the fluid in the horizontal direction but settling normal to the plane of fluid velocity and its gradient. Consider cases (i) and (ii) in detail.

The case (i) of a neutrally-buoyant particle is well studied, and observations date back to Poiseuille observing blood corpuscles aggregating on a certain ring in blood vessels [162]. It was studied in detail in [178] to demonstrate that particles aggregate on the equilibrium radius of $0.62R$ (this is called a pinch effect). Along these lines, there was a chain of theoretical studies elaborating on the lift force on a particle in this configuration, extending the applicability of this analysis in terms of the channel Reynolds number $Re_c = \rho U d / \mu$ from order unity [95] to large values [7] (U is a mean flow velocity, and d is the channel width, while ρ and μ are the fluid density and viscosity). The most recent results in this branch come from [114], observing equilibrium positions for neutrally-buoyant spheres in a tube flow at large channel Re_c and comparing the lab data with numerical simulations with account for the lift force obtained in [7]. The results of [7] were generalized for the flow in a circular pipe in [116].

For the special case mentioned above of a small sphere moving with a slip relative to linear shear flow (in the plane of velocity and its gradient, see Fig. 5a), an analytical expression

for the lift force \mathbf{F}_{lift} was obtained in [175]. The migration of a particle moving with a nonzero slip velocity in a shear flow of a viscous fluid is due to a small but nonnegligible fluid inertia. The "inertial lift" force is actually due to the inertia of the fluid, not that of the particle. There will be no migration in Poiseuille flow at vanishing channel Re_c . In terms of relative comparison of the lift forces, the lift force in the presence of the inter-phase velocity slip (the Saffman's lift force) is larger by one order of magnitude than the lift force on a neutrally-buoyant force-free particle rotating in a shear flow, so once there is slip, then rotation and its contribution to the lift can be neglected. The particles moving faster than the main Poiseuille flow will aggregate on the central axis, while the particles lagging the Poiseuille flow will be moving to the walls. The wall effect manifests itself in repulsing particles, so they accumulate at a distance from the wall [29, 31].

The Saffman force was later used in numerous applications, but the most relevant problem formulation to proppant transport was considered in [147], where a migration of proppant in the entry region of a fracture due to the Saffman lift force with a correction factor for the wall effects was studied. It was shown that, as a result of combination of particle slip velocity and the wall effect, particle-free near-wall layers are formed, and particles tend to accumulate on two planes away from the walls. An additional peak of concentration close to the fracture middle-plane is revealed due to the folding of the particulate sheet under the action of the lift force directed from the wall and the action of the virtual mass together with Archimedes forces on a particle in the boundary layer [147]. This solution is believed to be applicable in the entry region of the fracture, where the Poiseuille profile is being established: particles move faster than the fluid due to their inertia, and settling can be neglected

compared to longitudinal slip (see Fig. 5a).

Now we will consider the most relevant case (ii) typical of fracturing (see Figs.1 and 5b), where a single particle translates and settles in a pressure-driven flow of a Newtonian fluid through a vertical slot (slip normal to the plane of fluid velocity and its gradient). The expression for the lift force exerted on a particle in this configuration was obtained in [9]. This is the generalization of the Saffman force [175], taking into account three specific effects: the wall effect, particle settling, and local shear in the Poiseuille flow. The resulting force is acting from the fracture walls towards the fracture middle plane, so settling particles are expected to aggregate on the fracture middle-plane, leaving particle-free layers near the walls. These effects result in a non-uniform cross-fracture proppant concentration profile (recall that all conventional proppant placement models are derived under the assumption that the profile is uniform).

The 2D width-averaged model of particle transport in a fracture [29] for the case of a significant cross-flow particle migration was obtained by revisiting the derivation of the proppant transport equations from conservation laws and taking into account explicitly the non-uniform particle concentration profile when performing cross-fracturing averaging. A sensitivity study was performed and it was shown that migration to the fracture centerline results in higher proppant penetration lengths. The interplay between the lift force directed to the middle plane and the leak-off through the walls was further studied in [131]. It should be noted here that the work [85, 206] presented the 2D width-averaged model of proppant transport in the effective-fluid approximation [160], with analytical expressions for coefficients based on the assumption that all the proppant has migrated from fracture walls to the central core of the flow (forming a so-called "sheet flow"). The reasoning for migration mechanism was, however, different: the migration was due to visco-elastic properties of the fracturing fluid, based on experiments in visco-elastic fluid with particles in a pipe [203]. It is interesting that both visco-elasticity and settling in Newtonian Poiseuille flow through a vertical fracture result in the same migration from the walls towards the fracture middle-plane.

From above literature we conclude that all existing models of proppant transport assume that the cross-fracture particle volume fraction profile is uniform (exceptions being the recent studies by [29, 129, 51]). This implies migration is usually neglected. This assumption is only valid when the carrier fluid is a strongly cross-linked gel with a significant yield stress, so that the entire fracture cross-section is occupied by an unyielding plug of particle-laden suspension, with a slip on fracture faces (in this mental picture particles are frozen into the unyielded plug of the yield-stress fluid). Otherwise, there are forces in the shearing fluid moving particles across the fracture channel. Neglecting the cross-flow migration of proppant results in underestimating the penetration length and rate of sedimentation, which impacts the estimate for the propped fracture area. Based on the above reasoning, the existing simulators tend to underestimate the propped length and overestimate the propped height, because the sheet of proppant tends to move faster longitudinally (compared to the average flow velocity) and to fall quicker

because of gravitational convection effects (clean layers of fluid move up as heavy particle laden core settles down). The impact of migration on settling is similar to that of the Boycott effect of enhanced sedimentation in inclined fractures (see Sec. 5.3).

To summarize, the results for the lift force on neutrally-buoyant particles should not be directly applied to proppant transport. There is a fundamental difference between the results for the lift on proppant particles translating and settling in a fracture [9, 29, 206] and neutrally-buoyant particles translating in a channel or a tube [7, 114, 116]: the lift force in the presence of the slip is larger by order of magnitude, always directed from fracture walls to the middle plane and it does not have an equilibrium position anywhere except the channel centerline. This means the migration from the walls to the centerline continues until the particles form a rather concentrated suspension near the middle-plane of the fracture, and other forces peculiar to dense suspensions come into play. Eventually, a quasi-steady state non-uniform concentration profile is formed. The shear-induced migration in dense suspensions is reviewed in the following sub-section. A summary of prior art on lateral forces on a single spherical particle, published by the mid-2000s, is given in [115].

Migration in concentrated suspensions. Relevant to conventional fracturing is shear-induced particle migration in concentrated suspensions. A relevant two-phase mathematical model now ceases to deal with the individual particles, and migration is represented by the relative motion of the two phases. Constitutive relations are required to define the relative motion in terms of the particle concentration, the buoyancy force and the mean deformation rate gradient field. None such constitutive relations have been proposed for a fully 3D flow field, but restricted forms for near-unidirectional mean flows have been examined.

Existing particle migration models may be divided into two major classes: (i) the diffusive flux approach, in which migration is described in terms of particle diffusive fluxes and a diffusion equation, and (ii) the suspension temperature (or suspension balance) approach. The difference between the two approaches is in the expression for the suspension stress tensor and closure relations. All approaches to modeling of shear-induced migration in concentrated suspensions are developed for *neutrally-buoyant* particles, while proppant typically settles with a non-negligible slip velocity (unless it is trapped in the unyielded plug flow of a cross-linked gel, for which migration phenomena less relevant).

Diffusive flux model. The diffusive flux model was first suggested in [4] in order to explain the change in the viscosity of a concentrated suspension in the shear flow in a Couette rheometer observed in [72]. The model was then extended to more general two-dimensional flows [161]. To describe the diffusive particle migration, an effective continuum (fluid with particles) was introduced with the mass-averaged (or volume-average) suspension velocity. In our case of neutrally buoyant particles the mass average is equivalent to the volume average, and the suspension velocity field is non-divergent for an incompressible suspending fluid.

Boundary conditions consist of the no-slip velocity condition

on solid surfaces. This assumption may be justified as boundary regions with high shear rates are expected to be zones with low particle concentration and, therefore, there is only a small residual influence of particles on the no-slip condition. Following [161], assume that particle diffusive fluxes are based on two-body irreversible interactions between particles. However, for high C_p , the inter-particle interactions are not two-body, but multi-body, which makes the problem nonlocal. The number of collisions for a test particle in a shear flow scales like $C_p \dot{\gamma}$, where $\dot{\gamma}$ is the mean local shear rate. The variation of the collision frequency on the scale of the particle size a is given by $a\nabla(C_p \dot{\gamma})$. If the migration velocity is linearly proportional to this variation and every interaction provides a drift $O(a)$, then the particle flux N_c due to this effect can be specified in the following form:

$$\mathbf{N}_c = -K_c a^2 C_p \nabla(C_p \dot{\gamma}) \quad (12)$$

As a result, particles migrate to the regions of lower shear rate. Another particle flux is related to the gradient of the suspension viscosity, which results in resistance to the particle motion. This effect causes the displacement associated to each particle-to-particle interaction to be proportional to the change in viscosity over a distance $O(a)$ multiplied by the particle size: $a(a/\mu_s) \nabla \mu_s$. Taking into account the interaction frequency scaled as $C_p \dot{\gamma}$, we obtain the total flux N_μ to the region of a lower viscosity:

$$\mathbf{N}_\mu = -K_\mu C_p^2 \frac{a^2}{\mu_s(C_p)} \frac{d\mu_s}{dC_p} \nabla C_p \quad (13)$$

Once the fluxes are defined, the evolution equation for C_p can be written as:

$$\begin{aligned} \frac{dC_p}{dt} &= -\nabla(\mathbf{N}_c + \mathbf{N}_\mu) = \\ &= K_c a^2 \nabla(C_p \nabla(C_p \dot{\gamma})) + K_\mu a^2 \nabla \left(\frac{\dot{\gamma} C_p^2}{\mu_s} \frac{d\mu_s}{dC_p} \nabla C_p \right) \end{aligned} \quad (14)$$

The boundary condition is zero flux of particles on solid surfaces $(\mathbf{N}_c + \mathbf{N}_\mu) \cdot \mathbf{n}_{surf} = 0$. In the evolution equation for C_p (14), there are two non-dimensional coefficients K_c, K_μ , which are assumed constant, and there is no evidence from experiments that these are intrinsic functions of other flow parameters. These coefficients are phenomenological parameters, determined from comparison of model predictions with lab data or direct numerical simulations (DNS). In [161], the model was compared with experiments, and the best fit was found for $K_c = 0.41, K_\mu = 0.62$.

Suspension balance model. An alternative approach to modelling the shear-induced migration is the so-called suspension balance model (SBM) or suspension temperature model, based on kinetic theory of granular flows [75]. In [128], SBM is based on conservation equations for the suspension and the particulate continua, with the phase velocity introduced by:

$$\mathbf{v}_p = \langle \mathbf{v}_p^{real} \rangle, \quad \mathbf{v}_p^{real} = \mathbf{v}_p + \mathbf{v}'$$

Here, \mathbf{v}_p^{real} is an actual particle velocity and \mathbf{v}' is a fluctuating velocity due to inter-particle interactions. To define the pressure of the particulate phase p_p , the suspension temperature is introduced as a measure of chaotic motion of particles, in a similar way as in the kinetic theory of dense gases: $T = \langle \mathbf{v}' \cdot \mathbf{v}' \rangle$. The pressure for particulate medium can be then introduced as [128]:

$$p_p = p_0 + \mu_f \sigma^{-1} p(C_p) T^{1/2}$$

Here, σ is the mean free path between inter-particle collisions, and $p(C_p)$ is a non-dimensional function of the volume fraction; its form can be derived as follows. The evolution equation for granular temperature stems from the energy conservation equation:

$$\rho_p C_p c(C_p) \frac{dT}{dt} = \sum_p : \mathbf{e}_p - \mu_f \alpha(C_p) \sigma^{-2} T - \nabla \cdot \mathbf{q} \quad (15)$$

In (15), the first term on the right-hand side is the rate of work performed by the stress, the next term is the fluctuation dissipation, and the last term is the divergence of the heat flux vector \mathbf{q} . The non-dimensional functions $\alpha(C_p), c(C_p)$ and the vector \mathbf{q} have also to be specified from experiments or from direction numerical simulations (e.g., Stokesian Dynamics). The pressure function was suggested in the form [128]:

$$p(C_p) = C_p^{1/2} \left[\left(1 - \frac{C_p}{C_{max}} \right)^{-2} - 1 \right]$$

which includes the asymptotics $p(C_p) \sim C_p^{3/2}$ as $C_p \rightarrow 0$ (and $p_p \sim C_p^2$ for $T \sim C_p$ as $C_p \rightarrow 0$) and diverging $p(C_p) \sim 1/(C_{max} - C_p)^2$ as $C_p \rightarrow C_{max}$ (where C_{max} is a maximum packing fraction).

The heat flux vector \mathbf{q} is typically assumed to be governed by the Fourier law:

$$\mathbf{q} = -\mu_f k(C_p) \nabla T, \quad k(C_p) = k_k \mu_s / \mu_f$$

Here, k_k is a numerical constant. In a fully developed flow, $\partial T / \partial t = 0$, so there was no need to define $c(C_p)$ in [128]. The function $\alpha(C_p)$ is used in the following form with another numerical constant k_α :

$$\alpha(C_p) = k_\alpha C_p^{-1} \mu_s / \mu_f$$

The numerical constants k_k and k_α have to be obtained from experiments or DNS. In [128] these constants were found to be $k_\alpha = 0.19, k_k = 0.17$. To close the model, a symmetry condition at the channel middle-plane, the no-slip condition and the vanishing temperature at the solid wall were specified as boundary conditions.

The paper [62] shows the results of application of the suspension temperature model to shear-induced particle migration across a hydraulic fracture, which yields a significantly non-uniform cross-fracture concentration profile, with a maximum at the center-line. The author also argues that cross-flow migration intensifies sedimentation.

The SBM was recently revisited in [145], highlighting some inconsistency in the original formulation recently pointed out

by [132]: shear induced migration was believed to be driven by the divergence of the particle phase stress, but the latter does not explicitly enter into the volume-averaged momentum balance equation of the suspension. The authors argue that the hydrodynamic part of the particle phase force should be written as the sum of an inter-phase drag and the divergence of a hydrodynamic particle phase stress (the latter is shown to drive migration). Exact expressions for these quantities are derived from micromechanical considerations. The authors, in particular, make a very important conclusion: the particle phase pressure or any component of the particle phase stress tensor cannot be determined directly from rheological measurements of the suspension.

Migration in visco-elastic fluids. Experiments, e.g. [99, 74], demonstrate that in power-law fluid ($n < 1$) particle migration is towards the wall of pressure-driven tube flow, while for a highly elastic liquid the migration is towards the tube centerline. Experiments by [203] on particle motion in Poiseuille flow of visco-elastic fluids (spherical particles in crosslinked HPG fluids typical of hydraulic fracturing) showed that particles migrate laterally due to normal stress gradient on the particle scale. The summary of findings is as follows [203]: weakly cross-linked fluids that have shear-thinning properties with non-zero normal stresses over the range of shear rates produce rapid migration to regions of lower shear rate, i.e., the pipe axis. Polymer gels with higher levels of crosslinking produce little or no migration. This is due to the yield stress resulting in plug flow and wall slip. At lower values of the Weissenberg number $We < 5$, there appears to be a linear relationship $v_L \sim a^2 We \partial \dot{\gamma} / \partial y$. Once C_p reaches ~ 0.3 , migration rate significantly reduces, as the impact of particle-particle interactions becomes sufficient to resist the normal stress gradient driving the migration. The work [89] presented the calculation of the lift force on a particle in the Poiseuille flow of a second-order fluid (Tab. 3). There is also a bulk body of literature of direct numerical simulation (DNS) [96] of particle motion in visco-elastic fluids using contemporary numerical techniques, e.g., including lattice-Boltzmann modeling (LBM) or smoothed particle hydrodynamics (SPH) for fluid flow around particles coupled with FEM for solids). These DNS methods could provide a way of evaluating lift forces on a particle in complex fluids, which could then be used as closure relations in continuum models of suspension flows.

2.4. Interfacial instabilities

During alternate-slug fracturing, the displacement of a highly-viscous yield-stress suspension by a lower-viscous clean gel gives rise to the development of the Saffman-Taylor instability [174]. This instability can be both dangerous to the treatment when uncontrolled, or may help optimize hydraulic fracture conductivity, e.g., when used to create highly conductive fractures with channels supported by pillars [31], optimize an overflush stage at the end of stimulation treatment [117, 155], or place barriers to the fracture top and bottom for height growth control [148].

Usually, highly conductive channels in a propped fracture are achieved via heterogeneous proppant placement as a result

of alternate-slug pumping. Another methodology of achieving the same may be based on using the Saffman-Taylor instability mechanism and properly selecting fluids and slurries in a pumping sequence (see Fig. 6 for illustration of the pattern of pillars resulting from instability). In overflush, fingering helps prevent fracture closure and pinch-out in the near-wellbore zone, thus keeping the fracture hydraulically connected to the wellbore [153, 155].

Another remarkable example of using the Saffman-Taylor instability in hydraulic fracturing is the barrier placement for hydraulic fracture height growth control [148]. A method for placing a barrier at the bottom or the top of a hydraulic fracture to control the undesired growth of the fracture height is based essentially on the penetration of a finger of a low-viscosity fluid into a high-viscosity suspension in a fracture due to the Saffman-Taylor instability, thereby cutting the higher-viscosity slurry into two slugs, which are then displaced to the top and the bottom of the fracture. These pillars, upon reaching the fracture tip at the top and bottom, cause a premature tip screen-out (TSO), thus preventing the excessive fracture height growth.

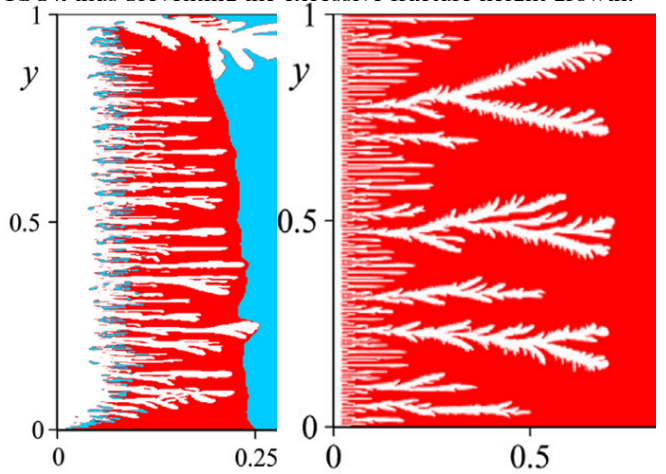


Figure 6: Fingering in sequential displacement of three fluids (yield-stress suspension – red, linear gel – blue, water – white) (left); fractal-like fingering in displacement of yield-stress suspension by water (right). After [31].

Another set of good lab data is presented in [182]: 89% glycerol solution displacement by water, and 1% polyethylene oxide (PEO) solution displacement by water with proppant. The resulting fingering patterns could be a very good set of data for validation of 2D proppant transport codes, but, to our knowledge, these data were only used for calibrating 1D mixing length models so far. Overall, fingering as a result of fluid sequencing in a fracture is quite widely reported in the literature, but only in rare cases are these numerical results validated (e.g. [194]). At the same time, it was demonstrated [31, 153] that the development of a predictive model is only possible in comparison with lab tests, as the particular width and length of fingers, which govern the development of the mixing zone, is heavily dependent on fine details of the numerical implementation. This illustration emphasizes the importance of model validation vs. real data from experiment. Important of fingering is re-emphasized in Sec. 4.2 on flowback and cleanup of propped fractures.

2.5. Leak-off

Leak-off is the term referring to the outflow of the fracturing fluid from the fracture through permeable fracture faces into the ambient reservoir during treatment. It is a very important phenomenon, which affects proppant transport on several length scales, from the bulk mass conservation to particle migration across the fracture width. In this subsection, we will briefly discuss the developments of leak-off models, from Carter's approach through pressure-dependent models to the most complex case of imbibition in shales.

Carter's formula. The most widely used model for leak-off is the Carter's formula for the leak-off velocity, which is obtained as an analytical solution of the fluid flow problem for a semi-infinite porous medium [38, 57] (the first reference appears in appendix to [94]):

$$v_L = \frac{2C_L}{\sqrt{t - t_0}}$$

A review of classical leak-off models is given in [179]. The Carter's model breaks down, at least, near the tip of the fracture, mostly because the leak-off velocity is no longer normal to that of the main flow, and in the areas where proppant is packed (bridging, jamming).

Extensions to Carter's model. Extensions to Carter's model include transient modifications, where the fracturing operation is split into two different stages in terms of the volume of fracturing fluid injected, with the threshold being the volume of fluid loss required to allow formation of a steady-state external filter cake on fracture surfaces (called the spurt loss) [217]. Until filter cake is formed, the leak-off is transient according to Carter's law, and its rate is governed by the permeability of formation. Once the filter cake reaches equilibrium, the leak-off becomes steady-state, determined by the resistance of the cake to the flow of fracturing fluid. A fully pressure-dependent leak-off model is not yet an industry standard for fracturing simulators, as it basically requires to have a separate module for flow in porous medium (multiphase filtration in the matrix, internal filter cake growth in the pores, and external filter cake buildup on the fracture surface), which would be linked to the proppant transport module through pressure continuity boundary condition on the fracture face. A predecessor of the model along these lines was presented in [158], where an experimental study of leak-off for various fracturing fluids was carried out and a theoretical framework for a combined leak-off coefficient was given. Several fluids were considered: BCLG (borate-crosslinked-guar), linear-guar, linear HEC (hydroxyethylcellulose), VSS (viscoelastic-surfactant solutions). Based on the Williams equation (originally derived for Newtonian fluids), a generalization is proposed for the leak-off coefficient for power-law fluids under the assumption of a piston-like displacement of the compressible fracturing fluid into surrounding formation.

Further extensions to model leak-off in shales. Leak-off is the problem of a moving front of liquid into the nanoporous matrix filled by gas, hence we need to be able to model the flow of liquid and gas in shales. Leak-off is closely linked with flowback, as the former provides initial conditions for the latter. In nanoporous rocks, the continuum approach breaks down

and the condition $\text{Kn} \ll 1$ is no longer valid, so that Darcy's law is not applicable. In terms of the Knudsen number, one can distinguish several flow regimes: the free molecular regime ($\text{Kn} > 10^{-1}$, and molecular dynamics methods are applicable) or the slip effects ($10^3 \leq \text{Kn} \leq 10^1$, and correction to permeability can be used in the form: $K_s = K(1 + K_b/p)$, where K_b is the Klinkenberg constant [101]). The non-Darcy flow regime in shales was stressed in the work [219], which presents a comprehensive model for gas transport that converges to a diffusion-type equation based on the modified Darcy law with a correction to permeability with the Klinkenberg constant due to slip effects.

As for the flow of the fracturing fluid into the formation, the study [169], based on the lab-scale experimental data, revealed that for realistic apertures of the main hydraulic fractures over time scales typical of the field job, a significant fraction of the injected fluid can be absorbed by the shale. Several flow channels within the shale system have been identified, including microfractures conductivity, matrix permeability, and the permeability in the vertical direction.

Thus, not only Darcy's law fails in shales due to ultra-low porosity and permeability, but also the mechanism of leak-off fundamentally changes from liquid flowing out into the pores (as in conventional highly permeable rocks) to liquid sinking into natural fractures and then slowly imbibing the low-permeability matrix. The effect of natural fractures on leak-off was widely discussed in the literature, e.g., [19]. Pressure-dependent approaches were considered [16], but no consensus has been reached yet on what model should be used to describe leak-off in shales.

3. Particle-laden flows in wells when pumping a fracturing job

The goal of recent research on the topic was to develop a model of the transport and dispersion of a slug of fiber-laden slurry in a well with application to the fracturing technology involving heterogeneous proppant placement, where slugs of proppant laden slurry are alternating with slugs of clean fluid. There is prior art in this domain, which is very well summarized in the literature review presented in the thesis [91]. Generally, the transport and dispersion of slugs is modelled within the 1D approach, assuming the flow is turbulent, and the axial dispersion (the evolution of cross-section averaged solids concentration C_p) is governed by the following non-linear convection-diffusion equation:

$$\frac{\partial C_p}{\partial t} + \frac{\partial F}{\partial x} = \frac{\partial}{\partial x} \left(\varepsilon_p \frac{\partial C_p}{\partial x} \right) \quad (16)$$

Here F is a convective flux taking into account transport of solids by mean flow and settling and ε_p is a total diffusivity coefficient. Diffusion in the axial direction is considered to be caused mainly by the Taylor dispersion [202]. The carrier fluid is shear-thinning with yield stress and can be described by the Hershel-Bulkley rheology model. Such a model takes into

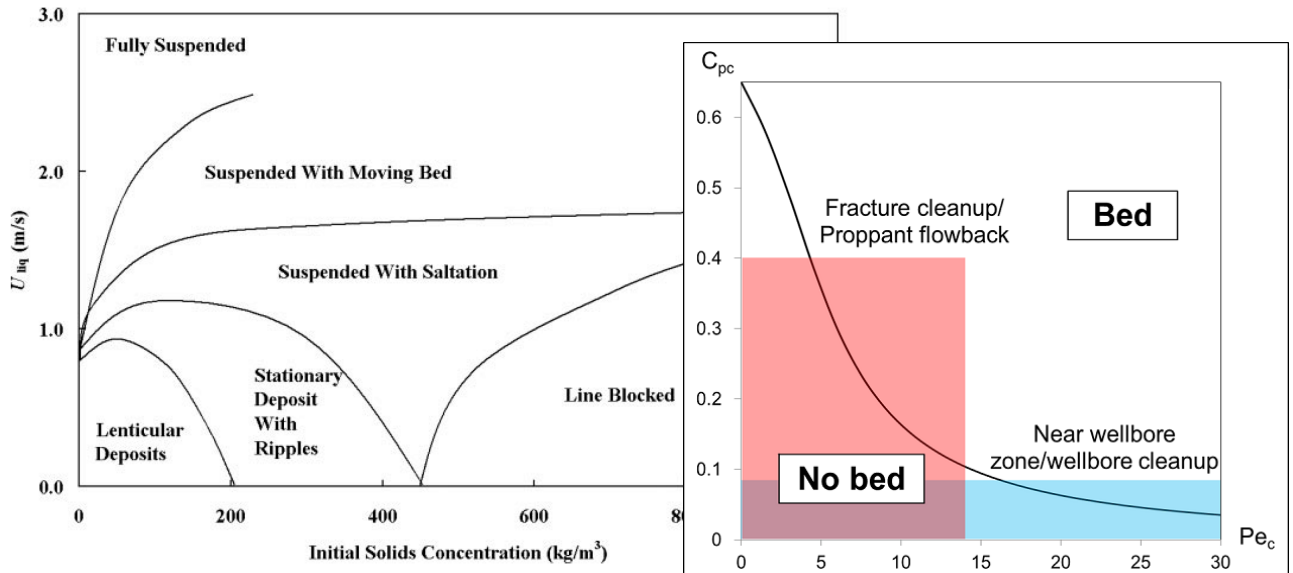


Figure 7: Flow regimes in a near-horizontal pipe flow of suspension (monodisperse $60 \mu\text{m}$ glass beads in 20 mm diameter pipe), after [146] (a). Flow pattern map in the C – Pe plane and critical curve separating flow regimes with/without bed formation (b). $Pe_c = v_s/UD\varepsilon_p$.

account effects of particles on suspension rheology and cross-sectional velocity profiles. An empirical relation for eddy particle diffusivity is needed to close the described model.

We distinguish at least two different approaches to developing the closure relation for the total diffusivity coefficient ε : (i) the homogeneous slurry (Reynolds analogy) approach, which basically treats the slurry as a homogeneous effective fluid, modeled locally with an effective viscosity, so that the Reynolds analogy is applicable [202], [40], [113], [156], [91], [92], and [93]; and (ii) the approach to suspension flows with higher particle inertia, where the key mechanism is axial dispersion, but the particle dispersivity is different from the diffusivity of the main fluid [213], [60], [61], [63], [192]. This approach takes into account the inertia of the particles, assuming the spectral energy density distribution of eddies, but modifying the range of the spectrum according to particle size/separation considerations (small scale cut-off increased by the presence of particles, as pointed out in [91]).

Reynolds analogy may be applicable only for very high-viscous liquids and fine particles. It seems to be appropriate for modeling of cross-linked gel only. Semi-empirical correlation from [63] is validated only for water and a certain range of particle diameters and could not be extrapolated out of the validated range of parameters [91]. Information on correlations for particle diffusivity ε_p is summarized in Table 4, where f_{sl} is the slurry friction factor, r is a radial coordinate, ρ_{sl} is the slurry density at a given point, $\bar{\rho}_{sl}$ is the cross-section averaged slurry density, τ_s is the particle relaxation time, and T_L is the fluid Lagrangian time scale.

The model [63] is focused on vertical pipes and does not cover the cases of fiber-assisted transport of solids. Taylor dispersion is supposed to be the only potential mechanism of slug dispersion. However, in horizontal pipes the dispersion may be caused by segregation of the suspension in the cross-section as well. The presence of fibers noticeably changes the flow structure. Fiber networks suppressing both particle settling and turbulence may also alter the key dispersion mechanism.

3.1. Areas for future work on solids transport in wells

Future research efforts on the development and validation of a 1D model for the transport and dispersion of fiber-laden slugs of slurry in a deviated well during proppant placement should be focused around the following aspects.

Mixing at the interface between a mixture slug and a clean fluid. Existing models of slug transport down the well are based on the concept of Taylor dispersion, essentially using the assumptions of turbulent flow regime in a Newtonian fluid. At the same time, there is evidence that fiber-laden suspension of proppant in fracturing fluid exhibits strongly non-Newtonian rheology (yield stress). Accurate prediction of the flow regime inside and outside of the slug is crucial for understanding the dispersion at the interface between the slug and the clean fluid. Understanding the physics of mixing between fiber-laden suspension and clean fluid during transport down the well is a key to control the slug transport from surface to perforations. The goal of the technologies of heterogeneous proppant placement is to make sure the slug is delivered to perforations intact with minimum dispersion, and then placed inside the fracture to create a stable pillar to keep the fracture open after the end of the treatment. On the contrary, massive dispersion of the slugs in the well eventually smears a sharp boundary between the slugs and a clean fluid inside the fracture, which leads to the loss of hydraulic conductivity of the propped fracture after closure (less amount of open channels between pillars in a closed fracture). Potential phenomena responsible for the mixing mechanism are: gravity segregation in cross-section of a near-horizontal pipe/suspension destabilization; longitudinal diffusivity due to turbulent Taylor dispersion; viscous fingering, development of Kelvin-Helmholtz instability at the interface stretched along the streamlines; flocculation and slip of solids admixtures.

4. Flowback from fractured wells during startup and testing

Once the fracture network is created as a result the hydraulic fracturing treatment, pumping is stopped, pressure is lowered,

	Homogeneous slurry/Reynolds analogy [202, 91]	Particle dispersivity [63]
Correlation	$\varepsilon_p = 0.0556 \sqrt{f_{sl} r} \left(1 - \frac{2r}{l} D\right) U$	a. $\varepsilon_p = 0.292 \left(\frac{d_p}{D}\right)^{0.32} \left(\frac{\rho_{sl}}{\rho_{sl}} f_{sl}\right)^{2/3} \left(1 + \frac{\tau_{sl}}{T_L}\right) DU$ b. $\varepsilon_p = 0.065 \left(\frac{d_p}{D}\right)^{0.32} \left(\frac{\rho_{sl}}{\rho_{sl}} f_{sl}\right)^{2/3} DU$
Validation	Salt solution in water	Sand in water without fibers
Potential application	High-viscous cross-linked gel	Slickwater

Table 4: Summary of particle diffusivity relationships.

and the fracture system is allowed to close under the action of confining stresses in the reservoir. The next stage in the life of a well is cleanup of the propped fracture network and the well from the fracturing fluid. This stage is conventionally called flowback. The key controlling parameters for flowback are the choke size and the back pressure on surface (see, e.g., [183]). The nuance of flowback execution in the field is that the stimulation treatment and the flowback operation are usually not coordinated in terms of a unified design. As a result, the added value of the well created by stimulation is sometimes lost at the stage of flowback [216], when the well is flowed back at excessively high rates, which creates excessive drawdown in the reservoir towards the fracture (resulting in tensile rock failure) and inside the propped fracture (resulting in proppant flowback). These undesired geomechanics events sometimes result in fracture closure and pinch-out in the near-wellbore zone, which leads to the loss of hydraulic connection between the fracture and the well [164]. Similar risks are posed by overflush during placement [155].

The next stage after flowback is transient pressure testing, which is a very well studied domain. A comprehensive review can be found, for example, in [105]. The specific features of well testing in the case of a horizontal well can be found in [104]. Transient pressure testing in fractured reservoirs using a DFN model is presented in [106]. The concept of coupled modelling the near-wellbore and wellbore cleanup with application to cleanup after drilling is given in [204]. The integrated approach to modeling of flowback in the fracture system and the well after the end of stimulation is proposed very recently [164].

In the case of flowback from multistage fractured wells, the problem is essentially a coupled one, integrating the 3D flow in the reservoir into the fracture (displacement of fracturing fluid by hydrocarbons in the matrix and bedding planes, natural faults, mineralized weak bedding planes), the 2D filtration in a propped fracture (displacement of the fracturing fluid by oil or gas), and, finally, a transient 1D gas-liquid flow in a deviated well. Modeling of flowback from fractured wells is not as mature as simulation of hydraulic fracture growth, and there is a room for more research in the field of flowback. Below we will briefly review the state of the art in flowback modeling in fractures and wells.

4.1. Flowback in fractures

Flowback in fractures (or a branching fracture network in shales) includes the following different stages: flowback of fracturing fluid (and, sometimes, suspended proppant) from the fracture system while fractures are closing on proppant (in this case the fluid is being 'squeezed' out of the system into the wellbore [214]) and the filtration in a closed propped fracture (or partially propped fracture system in shales), which is basically the problem of displacement of a fracturing fluid by hydrocarbons in a closely packed proppant inside fractures (or in fractures closed on asperities, in which case the conductivity is significantly lower).

The fracturing fluid has a specifically designed time-dependent rheology, which is shear-thinning while the suspension is pumped down the well, then it gains a yield stress due to delayed cross-linking of the polymer gel right before the mixture enters the fracture through perforations, and then the fluid gets shear-thinning again after fracture closure (due to the release of encapsulated breakers under closure stress, which degrade the polymer gel) to make the process of fracture cleanup more efficient.

The following phenomena are important: displacement of partially-cross-linked yield-stress fluid by hydrocarbons in propped fracture (the fundamental issue of cleaning up the proppant pack from gel residue) [13, 14, 194, 10], fines migration resulting in colmatation of the proppant pack in the near-wellbore zone and degradation of the fracture conductivity [27, 30]; displacement of fracturing fluid by oil or gas in the branching network of fractures (the major part of fracture network involves unpropped natural discontinuities closed on asperities and mineralized bedding planes); filtration in ultratight rock matrix. Accurate modeling of influx from an ultratight matrix into the fracture network cannot be carried out in the framework of traditional Darcy approach. In particular (as also noted in Sec. 2.5), Klinkenberg effects need to be taken into account in modeling of gas filtration in ultratight permeability matrix. The application of Darcy law would result in underestimation of fluid flow rates by several orders of magnitude [157].

In flowback, fluid mechanics and geomechanics phenomena are tightly interconnected, mutually influencing each other. From a geomechanics viewpoint, proppant embedment and plasticity of fracture faces under the action of confining stress,

as well as, tensile rock failure are key effects to be taken into account. The compaction of a proppant pack under the actions of a closure stresses on fracture faces within the classical Hertz contact theory was studied, e.g., in [73, 140].

Talking about fines migration in more detail, there are several sources of fine (small) particles during fracture flowback: crushed proppant; mobilized rock particles due to crushing/embedment/tensile rock failure; abraded rock minerals; abraded rock kerogen; solid polynomial residue; free precipitated inorganic scale (CaCO_3 , BaSO_4); waxes/asphaltenes [32]. The particle diameter ranges from several hundreds of micrometers (macroparticles, e.g., crushed proppant/rock) to sub-micron colloidal particles (e.g., inorganic scale, clay) [42]. Migrating particles typically damage the permeability of fracture, which leads to significant reduction in production rate of hydrocarbons. There is a family of well-established models for suspension filtration with effects of permeability damage and recovery due to particle trapping and mobilization, which are conventionally called the deep-bed filtration model. An overview of closure relations of this model for trapping and deposition can be found in [223]. The number of tuning parameters in these correlations is from one to five. The most frequently used correlation between the permeability and the concentration of trapped non-colloidal particles has the power-law form (see, e.g., [27]). For colloidal particles, the formula for trapping coefficient is obtained in [165] using a pore-scale micromodel of particle transport based on Happel's cell approach. The formula is valid only for particles not larger than several micrometers.

[86] proposed criteria for particle trapping due to direct interception, straining in constrictions and wedging in crevices. The trapping coefficient is claimed to be proportional to the initial porosity, particle and pore diameters, but the coefficient of proportionality is not estimated. In [78] and [86], particle mobilization or entrainment were studied. The key finding of these studies is that there exists a critical velocity of mobilization, above which particles are mobilized and the rate of entrainment is proportional to the concentration of trapped particles and the flow velocity. The coefficient of proportionality is a tuning parameter, which is called the mobilization coefficient.

Existing models for suspension filtration with non-colloidal particles contain two tuning parameters for describing the mobilization rate, and minimum of two other tuning parameters involved into the expression for the trapping rate. There are also emerging models developed within the multi-fluid approach (e.g., [30]), taking into account the filtration in large pore channels and, additionally, the flow in random close packing of trapped fine particles, which helps to reduce the number of tuning parameters in the model.

The challenge in modeling of flowback and cleanup of propped fractures is to come up with an approach that would cover the wide range of rich physics listed above, be validated and calibrated against experiments on core colmatation, and then this modeling workflow would allow one to determine a safe operating envelope for managing fracture flowback without undesired geomechanics events (such as rock failure, proppant flowback, conductivity degradation).

Proppant flowback. Experimental observations and numer-

ical results reported [125] seem to indicate that the bridging factor during flowback is higher than the typical value of 2.5. Indeed, they observe that the proppant does not mobilize if the fracture width is less or equal to 5.5 times the mean particle diameter. The sensitivity of the results to other parameters, such as confining stress, rock hardness, proppant roughness and proppant size distribution was relatively small. The numerical simulations performed by [6] (using the discrete element model, a predecessor of the well known PFC2D code) show results that are consistent with the experiments [125]. It was observed [6] that failure of the pack occurs when the fracture width is about 5.5 times the proppant mean diameter, and that the results are more or less insensitive to the confining stress and the contrast of elastic properties between the rock and the proppant. They also indicate that the pressure gradient along the fracture has a more significant effect on the results. Experiments [77] in a large scale slot emulating the fracture using large sand as proppant and water as the flowback fluid demonstrated that flowback is a strong function of fluid flow rate, particle size, fracture width, and closure stress, though not resulting in a particular correlation. A mechanistic model based on solid mechanics principles was presented as part of the complex study of proppant stability in [37]. The model was calibrated on a number of lab experiments on proppant pack stability, and then validated on field cases. It allows to obtain recommendations on a safe operating envelop in terms of the flow rate (choke size) allowable.

[118] conducted experiments on proppant flowback in big block tests with application to hydraulic fracturing for geothermal applications. Two configurations were considered: convergent radial flow and linear flow. Critical particle Reynolds number Re_c based on filtration velocity, particle radius and fluid density and viscosity was introduced to mark the threshold for proppant flowback to occur. $Re_c = 1.5$ and 6 were found for the linear and radial flow regimes, respectively. With the increase of the flow rate above a critical value (marked by Re_c), the conductivity in the radial flow regime was demonstrated to rapidly decline due to inertial effects and fines migration leading to colmatation. Wormhole channels were observed to develop in an overall stable proppant pack in the radially converging flow test.

At the same time, with limited mechanistic models available, current versions of proppant transport simulators use a constant de-bridging factor of ~ 5 during flowback. This geometric criterion needs to be replaced by a more realistic relationship that includes confining stress, rock hardness, proppant roughness, proppant embedment, and flow rate.

4.2. Gas-liquid flows in wells

The topic of gas-liquid flows in wells in itself is a very rich and complex domain, which deserves a separate detailed review. Here, we will only summarize the challenges peculiar to dynamic multiphase flow modeling relevant to flowback from a fractured well. A comprehensive review of the state of the art in multiphase flow modeling can be found in the book [35].

One of the most dangerous flow regimes, threatening the integrity of the propped fracture network, and the most difficult to model numerically is the slug flow regime during a gas-liquid

flow in a near-horizontal well. The gas-liquid slug flow can form due to either terrain-induced slug flow (due to low elbows in the near-horizontals), or hydrodynamically induced (Kelvin-Helmholtz instability at the interface between gas and liquid in stratified flow), or might be due to degassing in the vertical section (aggregation of bubbles leading to large Taylor bubbles). The slug flow is an alternating flow of relatively large portions (slugs) of pure gas and pure liquid, which is characterized by oscillating pressure at each point along the pipeline and peaks of mass flow rate on surface. Pressure oscillations on perforations may damage the near-wellbore zone resulting in proppant flowback, tensile rock failure, and pinch-out, disconnecting the fracture from the wellbore, as outlined above, or in proppant crushing due to fatigue – also leading to loss of fracture-to-well connectivity. Figure 4.2 illustrates the peculiarities of the terrain-induced slug flow in a near-horizontal pipeline, where gas is injected at the inlet and liquid is supplied around the left lower elbow (configuration studied in [48]).

In the industry, there are a number of commercial simulators based on the full multi-fluid model (the multi-continua approach to multiphase flow, using separate momentum conservation equations for each phase) and the simplified drift-flux model (using a single momentum conservation equation for the mixture and explicit algebraic relations for phase velocities via the mixture velocity and the slip velocity). Examples of the multi-fluid model implementation include the pioneering simulator with a Lagrangian slug-tracking approach to modeling of slug flow regime [24] and the models introduced relatively recently using an Eulerian slug-capturing technology [98], [47]. Slug-tracking approach is based on semi-empirical correlations for slug appearance and decay, and closures for the velocity of the slug head and tail. This approach, being calibrated on a vast amount of lab data, allows one to simulate complex flows on relative rough meshes with acceptable computational speed. In contrast, the slug capturing approach is based on modeling the slugs directly, which requires very fine meshes, and hence is computationally much more expensive. Yet, with the recent progress in parallelization techniques (both multi-CPU and multi-GPU) the cost of slug-capturing simulations becomes affordable. There is a family of research codes implementing the slug-capturing technology, e.g. [97], [152], [200].

In the multi-fluid model, there is also a fundamental issue with hyperbolicity of the model and well-posedness of the boundary-value problem [222]. Most multi-fluid models used in the industry are conditionally hyperbolic. Loss of hyperbolicity results in unphysical artificial oscillations in the numerical solution and in loss of grid convergence [97], which, at best, does not allow one to get a solution of fine meshes, and at worst, results in divergence of the numerical algorithm. Drift-flux models also suffer, although the issue is less pronounced [222].

The success in application of the drift-flux model to modelling quasi-steady-state three-phase gas-oil-water flows in near-vertical wells is essentially based on calibration of the drift-flux correlations for phase slip velocities on extensive lab data [186, 187]. The drift-flux model is also very stable and robust in terms of numerical implementation [64, 65, 66]. The

de
try

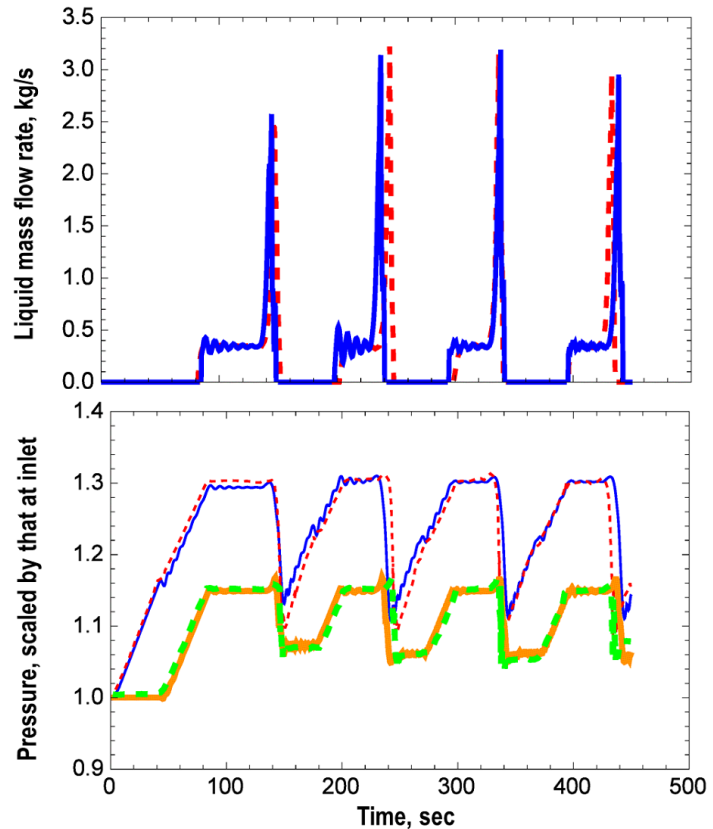
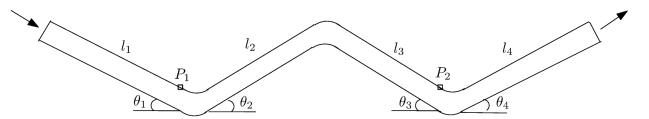


Figure 8: The sketch of the slug flow in a near-horizontal W-shaped well, after [48] (a). Gas-liquid slug flow regime characterized by pulses of mass flow rate at outlet (b) and pressure oscillations at points P1 and P2 (c) vs. time. Dashed line – experiment [48], solid line – drift-flux simulation [196]. After [196].

Surprisingly enough, the drift-flux model, originally developed to model quasi-steady-state production and known to be not suitable for modeling of hydrodynamic slugs (resulting from Kelvin-Helmholtz instability at the gas-liquid interface in near-horizontal wells), is capable of simulating the terrain-slug flow regime (see Fig. 4.2). The reason is as follows: the terrain-slug regime consists of two very different interchanging phases: a slow quasi-steady state segregation of gas and liquid in segments and a fast transient outflow through the entire well. First, gas and liquid are segregating in each inclined segment of the pipe, that is well captured by the drift-flux correlations, which stem from the problem of bubbles rising in liquid. Second, once the segregation in each segment is complete and gas pressure builds up enough to push out the mass of liquid from lower elbows, a highly transient outflow forms, which gives rise to peaks of mass flow rate of liquid at the outlet (Fig. 4.2). Yet, this transient outflow phase is essentially single-phase, because

gas and liquid are macroscopically separated into interchanging slugs, which is again well described by the single momentum conservation equation for the mixture with a step-wise uniform distribution of properties along the pipeline (numerical issues would arise when there are two momentum conservation equations for each phase, and degeneration of one phase leads to singularity in velocity distribution, unless regularized [152]). Once the pressure decays, the outflow stops and the regime switches again to gravity segregation of gas and liquid. Similar results can be, of course, obtained using multi-fluid models [24, 47, 98, 152], for which the slug-flow regime (hydrodynamic or terrain-induced) is a natural domain of applicability. Enhancements to the drift-flux model implementation in Lagrangian variables are presented in recent works [111, 111].

A coupled fracture-wellbore cleanup simulator is underway, utilizing in the wellbore section the drift-flux model, which proved capable of capturing the key relevant flow regime of gas-liquid terrain-induced slugs [164].

5. Constitutive relationships

There are a number of incoming factors, which affect closure relationships for the models of proppant placement and flowback, namely: drag reducers added into the fracturing fluid to minimize pressure drop along the well while pumping, flow rate which governs the flow regime (from laminar through intermittent to fully turbulent), polydispersity of proppant, non-spherical shape of proppant particles, addition of fibers to mitigate undesired settling of proppant. These factors affect both the bulk rheology of the slurry and the rate of longitudinal transport and sedimentation of solids.

The following phenomena require specific attention: dynamic bridging and mobilization of particles due to local dehydration (because of leak-off) or packing at the bottom (due to settling), local expansions or constrictions of the fracture channel, bridging at fracture turns and junctions with pre-existing faults; impact on sedimentation/segregation/in-situ channelization; clustered settling, clogging of particles and fibers, agglomeration; transition to packing limit, advanced models based on granular mechanics [34, 129, 130]; visco-elastic rheology of fracturing fluids, time-dependent response to shear, anomalous particle sedimentation effects; rheology of fiber-laden suspensions; polydispersity and its impact on rheology and sedimentation.

In order to mitigate the undesired effects of proppant settling in the near-wellbore zone (which typically reduces the propped area of the fracture), fibers have been introduced into the fracturing fluid composition to stabilize and consolidate the suspension [76]. The use of fibers already resulted in development of breakthrough technologies in proppant placement [69, 121]. At the same time, it is *the effect of fibers* that probably is the one mostly missing in the proppant transport modules of fracturing simulators. We will illustrate this fact below in respective subsections related to solids sedimentation and suspension rheology.

5.1. Settling

Sedimentation is probably the most studied subtopic in the entire theme of proppant transport, for two reasons. First, it is easily examined experimentally, as static settling experiments can be arranged and instrumented with much less effort than, for example, large scale dynamic slot experiments. Dynamic settling experiments are still doable, for example under conditions of simple shear in a large-gap Couette rheometer (see, e.g., [170]). Second, on the theoretical side, an explicit analytical formula can be easily obtained under the assumptions that the settling is steady-state, the flow regime is creeping (Stokes flow, no inertia: $Re_p \rightarrow 0$), the motion is due to the balance of the Stokes drag force, the gravity force, and the Archimedes (buoyancy) force. The solution of this equation is known as the Stokes settling velocity for a single particle. For a review of settling in Newtonian fluids, we refer to [3]. Table 5 shows a description of the settling phenomena and dimensions of complexity. It only touches base on visco-elasticity (there is a zoo of correlations, including recent attempts to come up with a unified approach [181]), and it is completely missing the effect of fibers (mainly because this one remains "under consideration" by community).

As shown in Tab. 5, there are four dimensions of complexity for the proppant settling velocity: inertia of the flow ($Re_p \sim 1$), non-Newtonian rheology of the carrier fluid, dense suspension effects, and effects of the wall. The effects of inertia seem to be of practical interest only in the case of slick-water fracturing, where particle Reynolds number Re_p may be no longer small (this topic is well studied, there are correction factors due to finite particle Reynolds number, and a summary can be found in [142]), whereas the other dimensions of additional complexity will be considered in a more detail here as being more relevant. For power-law rheology typical of fracturing fluids, the Stokes settling velocity can be generalized (see Tab. 5). In the case of Herschel-Bulkley rheology, there is an unyielded core of the flow (no settling) and sheared near-wall layers, where the settling obeys the above formula for power-law. The effects of visco-elasticity remain to be a relatively less studied domain. There are attempts to study visco-elasticity effects qualitatively, leading to counter-intuitive results: settling rate increases with increase in the concentration (explained as being due to extra shear caused by particles close to each other) and slows down at higher shear rate [170]. There is also a visible aging effect observed in lab experiments: suspension left at rest in the lab, may suddenly show settling hours later, after being apparently stagnant for a considerable time.

It has been known from experiments on longitudinal transport and vertical sedimentation in slots with rough walls, that roughness hinders sedimentation and causes proppant retardation in horizontal transport [133]. The measurements of the impact of roughness on hindered settling and retarded longitudinal transport could be valuable input into proppant placement models. The tendency of particles for self-organization during settling was observed and investigated in [138], [139]. Another phenomenon manifesting itself in enhanced sedimentation in inclined fracture channels (Boycott effect) is also studied but

Effects				
Complexity	Inertia $\text{Re}_p \sim 1$	Non-Newtonian rheology	Hindered settling $C_p \sim 1$	Wall effects $v_s/v_{St} = g(h)$
	$\text{Re}_p \ll 1$	Newtonian $v_{St}^0 = \frac{(\rho_p - \rho_f)gD^2}{18\mu_f}$	$v_s = v_{St} \left(1 - C_p/C_{max}^j\right)^\alpha$	$\alpha = 4.7 + 19.5h, h = d/w$
		$C_D = 24/\text{Re}_p$		
		Power-law $v_{St} = \frac{(\rho_p - \rho_f)gD^{n+1}}{3^{n-1}18K}$	$\alpha = 5.5$ [142], $j = 0$ [167], 1[28]	$g(h) = 1 - 0.65h + O[h^3]$ [142]
	$2 < \text{Re}_p < 500$	Visco-elastic $v_{St} = v_{St}^0 \left(1 - 0.18(\text{Re}_p \text{We})^{0.19}\right)^{-1/2}$ [1]	More data in Table 6	
		$C_D = 30/\text{Re}_p^{0.625}$	$\alpha = 3.5$ [142]	$\alpha = 4.45\text{Re}_p^{-0.1}$ [142]
	$\text{Re}_p > 500$	$C_D = 0.44$	$\alpha = 2$ [142]	$g(h) = (1 - (h/2))^{3/2}$ [142]

Table 5: Various effects contributing to settling velocity of solids.

Formula for $F(C_p) = v_s/v_{St}$	Source
$1 - 6.55C_p$	Batchelor's formula[22]
$(1 - C_p)^2/10^{1.82C_p}$	[43]
$\alpha = 4.65$	Original Richardson-Zaki's [167]
$(1 - C_p)^\alpha$	[84]
$\alpha = 4.5$	
$\alpha = 5.1$	[79]
$\alpha = 5.5$	[142]
$(1 - C_p/C_{max})^\alpha$	Proppant transport [28, 29]
$\alpha = 5$	

Table 6: Various closure relationships for the correction factor accounting for hindered settling at $\text{Re}_p \rightarrow 0$.

not implemented yet into commercial fracturing simulators as a standard feature [144].

The effect of finite volume fraction of particles in dense suspensions (known as hindered settling) is accounted for via the correction factor $F(C_p) = v_s(C_p)/v_{St}$. Various closures for the hindered settling effect are shown in Tab. 6. The issue with the original Richardson-Zaki formula and its generalizations is that it does not vanish as particles settle to the bottom and form a packed bed (at $C_p \rightarrow C_{max}$). Basically particles fall through the bottom according to Richardson-Zaki's, instead of accumulating and forming a bed. To cope with this effect an empirical relation was introduced in the form of $(1 - C_p/C_{max})^\alpha$ and it was used successfully to model proppant transport and settling [85, 206] (validation against dynamic slot tests with bed formation was presented in [29]).

Bed formation and dune transport in fractures and near-horizontal wells. Dune transport of suspension in fractures during slick water treatments is believed to be the key driving mechanism of the placement [117]. In near-horizontal wells, packed bed may form both during placement (when fracturing fluid's rheology does not keep particles from settling) and during production, when there may form a flow of proppant (coming out of fractures due to flowback) and fine particles (both crushed proppant and formation fines). A comprehensive review of solids transport in low-concentration flows can be found in [197].

Dating back to the classical models of fracture [100], the existing mental picture of particle transport in fracture network in shales created during high-rate water fracturing treatments

is as follows [117]: particles settle in the primary hydraulic fracture and are then transported by re-suspension and saltation [11, 12]. Existing placement models for fracture network in shales are effective 1D, based on the three-layer structure of pure fluid/flowing suspension/stagnant packed bed at the bottom. Incorporating resuspension and bed-load transport along the lines of Bagnold's theory would be a major step forward.

The same is true for multiphase flow models for near-horizontal wells during flowback, where there is a well-developed family of 1D models for solids transport with bed formation and resuspension (e.g., [54]-[56]), which are not yet a part of the integrated modelling workflow for flowback.

Fibers' impact on settling. There is a significant body of literature on suspensions of fluid with fibers (e.g., [87, 82]), but there is much less understanding of the behavior of fiber-laden suspension in the presence of particles. It is known from lab observations that in the presence of fibers proppant forms clumps and the settling of proppant is hindered. Moreover, there is a number of empirical factors taking into account hindered settling effects caused by fibers, but these semi-empirical models are not unified yet. There have been attempts to include the effect of fibers on proppant settling [171], mainly highlighting the complexity of the issue and showing some scatter in the measurement results. In fracturing simulators, the effect of fibers on settling is taken into account via the modified (decreased) density of the proppant by an empirical factor, resulting in reduced settling velocity, which is far from being a well grounded, satisfactory approach. More laboratory effort seems to be required, supported by systematic use of the dimensionality theory to in-

terpret the results and micromechanical considerations to develop a modeling framework for the settling velocity in the presence of fibers.

5.2. Suspension rheology: effect of non-Newtonian carrier fluid

A fracturing fluid is typically an aqueous solution of a polymer [20], which explains its strongly non-Newtonian behavior that needs to be taken into account when modeling proppant transport. The first task is to represent the bulk rheology of the suspending fluid in the form of a tensor-valued constitutive equation, or rheological equation of state (REoS). The field variables involved are the stress tensor \mathbf{p} , which is usually decomposed into a deviatoric part $\boldsymbol{\tau}$ and a thermodynamic pressure p ($\mathbf{p} = p\mathbf{I} + \boldsymbol{\tau}$), and the rate of deformation tensor $\mathbf{e} = (\nabla\mathbf{v} + \mathbf{v}\nabla)$, where \mathbf{v} is the vector velocity. It is usual to restrict attention to simple fluids that respond, in terms of stress, only to the history of their rate of deformation, and not to any spatial gradients in either stress or rate of deformation. In dealing with liquids it is usual to treat them as slightly compressible. Let us narrow down our consideration to "fluids", which are understood in continuum mechanics as media for which the deviatoric part of the stress tensor depends on the rate of strain only, and does not depend on the strains themselves:

$$p_{ij} = -p\delta_{ij} + \tau_{ij}(e_{ij}), \quad e_{ij} = \frac{1}{2}(\nabla_j v_i + \nabla_i v_j)$$

Further simplifications can be made [159, 108]:

- For Newtonian fluid: $\boldsymbol{\tau} = \mu_0\mathbf{e}$
- For a generalized Newtonian fluid: $\boldsymbol{\tau} = \mu(|\mathbf{e}|)\mathbf{e}$. Within this class, we can find the Bingham fluid, the power-law fluid and the Carreau fluid models
- For visco-elastic fluids, based on convective forms of linear models using the dynamic modulus we will only mention the most widely known, namely the Oldroyd B (convected Jeffreys) model:

$$\boldsymbol{\tau} + \lambda_1 \dot{\boldsymbol{\tau}} = \eta_0(\mathbf{e} + \lambda_2 \dot{\mathbf{e}})$$

The REoSs are written in evolutionary rather than integral form because simulation is much simpler using evolutionary models.

– For thixotropic fluids, which take a finite time to reach an equilibrium viscosity when introduced subject to a change in shear rate, the viscosity μ_T is governed by an evolution equation of the form:

$$\frac{\partial \mu_T}{\partial t} + (\mathbf{v} \cdot \nabla) \mu_T = \mu_{T0} f_n(\lambda_T, \mu_T, \boldsymbol{\tau} : \mathbf{e})$$

where λ_T is a characteristic recovery time.

VES fluids are described [17] with a combination of the Oldroyd B and the thixotropic fluid model. Such REoS applies to any continuous flow field, whether transient or not. The most common rheological measurement consists in imposing a uniform steady-state simple shear (USSSF) with the shear rate $\dot{\gamma}$. This is sufficient to obtain μ_0 , $\mu(\dot{\gamma})$, η_0 or μ_{T0} from the measured shear stress $\boldsymbol{\tau}$. It is also possible to measure a difference of normal stresses.

Currently, the rheology models for base fracturing fluids in commercial fracturing simulators are as complex as the power-law model (e.g., [209, 218, 5, 25, 26, 124] and others). The yield stress of the slurry is now only incorporated into research codes (e.g., FracFlow [31] and SHAC [127]), mainly because the yield-stress behavior complicates numerical implementation, greatly increases the computational time, and finally, is difficult to validate (see the validation campaign in [31]). Visco-elasticity and especially its effects on proppant transport is not taken into account at all.

5.3. Suspension rheology: impact of particles and fibers

A comparison of various closure relationships for rheology of dense suspensions is given in [198] (see Tab. 7).

For the specific case of proppant suspensions in a fracturing fluid, it was shown [15] that $\beta = -1.5$. At the same time, studies of proppant transport in fractures within 2D width-averaged model [85, 206] used $\beta = -1.82$ [103]. For the case of non-Newtonian (power-law) fracturing fluids, experiments performed with polymer gel with different concentrations (from 0 to 0.35) of neutral-buoyant spherical beads as proppant are reported in [57]. The results of these experiments show that the power-law index n of the suspension does not depend on proppant concentration, while the consistency index K depends on the particle concentration in a similar manner as in the case of Newtonian fluid, with exponent being now the function of a power-law index:

$$K = K_f \left(1 - \frac{C_p}{C_{max}}\right)^{5n_f/2}$$

where K_f is the value of the consistency index for the clean base fluid.

Fibers. As far as we can judge, the effect of fibers on rheology of flowing particle-laden fluids is currently poorly understood. Pure suspensions of fibers only are studied to a greater extent. For example, the rheological properties of fiber-laden suspensions (normal stress differences) were investigated in [193]. It was derived from experimental observations that normal stress differences for suspensions of fibres are determined by short-range repulsive interactions. Due to the strong alignment of fibers with the flow direction, the repulsive interactions act primarily in the gradient direction and weakly in the flow direction. In [83], the effect of fibers on the rheological property of fracturing fluid was investigated experimentally to show that fibers form a quasi-3D network to increase the apparent viscosity of fracturing fluid. The increment in apparent viscosity relies heavily on the shear rate, fiber concentration, thickening-agent concentration and temperature. Higher increment in apparent viscosity is found at lower shear rate and higher fiber concentration. The addition of fibers enhances the shear-thinning behavior of the fracturing fluid.

5.4. Bridging and transition to close packing

Packing. The transition to close packing is understood in the purely geometric sense as the configuration when the particle volume fraction reaches a certain maximum limit, where all

Formula for $\mu_s(C_p)/\mu_f$	Applicability domain, C_p	Source
$1 + 2.5C_p$	$C_p < 0.05$	Einstein [58]
$1 + 2.5C_p + 7.6C_p^2$	$C_p < 0.2$	Batchelor [23]
$(1 - 3.5C_p)^{-2.5}$	$0 \leq C_p < C_{max}$	Roscoe [172]
$(1 + 1.25C_p/(1 - C_p/C_{max}))^2$	$0 \leq C_p < C_{max}$	Ferrini [68]
$1 + 2.5C_p + 10C_p^2 + 0.0019 \exp(20C_p)$	$0 \leq C_p < C_{max}$	Thomes [195], [176]
$1.125(C_p/C_{max})^{1/3}/(1 - (C_p/C_{max})^{1/3})$	$0 \leq C_p \leq C_{max}$	Frankel & Acrivos [67]
$\beta = -2.5C_{max}$	$0 \leq C_p < C_{max}$	Krieger [102]
$\beta = -2.5$	$0 \leq C_p < C_{max}$	Nicodemo [141],[107]
$\left(1 - \frac{C_p}{C_{max}}\right)^\beta$	$0 \leq C_p < C_{max}$	Maron [137]
$\beta = -2$	$0 \leq C_p < C_{max} = 0.64$	Barree & Conway [15]
$\beta = -1.5$	$0.01 < C_p < C_{max}$	Krieger [103]
$\beta = -1.82$	$0 \leq C_p < C_{max}$	Scott [177]
$\beta = -1.89$		

Table 7: Various closure relationships for suspension rheology: from dilute to dense suspensions.

particles are in multiple contact with each other and their volume concentration cannot be increased without mechanically breaking them into smaller pieces. While solids suspensions are transported through the fracture, packing occurs when particles settle due to gravity to the bottom of the fracture, or arching and bridging is formed in the areas, where the fracture is too narrow, blocking the subsequent motion of particles packing against that arch, or suspension dehydrates due to extensive liquid leak-off through the fracture faces. Random packing of spheres yields a maximum concentration of 0.65, which is known as the random close packing limit. Geometrical studies provide a limit of maximum packing concentration of monomodal spheres $C_{max} < 0.74$ [205], but that ideal configuration is practically unattainable. It is a common practice in the industry to assume the maximum packing concentration as that for random close packing: $C_{max}^{rcp} = 0.65$. At the same time, the initial loose pack of particles forms at lower concentrations, $C_m = 0.585$ [129]. In the range $C_m \leq C_p \leq C_{max}^{rcp}$, the suspension is no longer sheared, but is rather compacting due to particles re-distribution [129].

The key issue with the family of closures for slurry rheology in Tab. 7 stems from their form $\sim (1 - C_p/C_{max})^\alpha$: all of them diverge in the packing limit $C_p \rightarrow C_{max}$. In simulations, this discontinuity is typically regularized by stepping out of the singularity by a small ε and specifying a high but finite slurry viscosity $\mu_s(C_{max} - \varepsilon)$. In order to provide a more mechanistically grounded model for the rheology near the packing limit, an effort was made recently to develop a unifying approach to describe suspension rheology from dilute suspension through concentrated slurry to the packing limit. To characterize the rheology, the work [34] uses a new nondimensional group I called the viscous number and introduced by [39]. The viscous number I is given by the following formula based on a micromechanical consideration of timescales of the solid particles motion in a suspension: $I = \mu_0 \dot{\gamma} / -\sigma'_n$.

This is the ratio of the viscous shear stress in the fluid to the particle confining stress. Based on rheological experiments performed under effective normal stress control on suspensions of monodisperse spheres in Newtonian fluids, the following phenomenological relation was proposed based on the combination

of the friction coefficients for the flowing and for the contact regimes $\mu_s = \mu^{cont} + \mu^{hydro}$ [34]:

$$\mu_s(I) = \underbrace{\mu_1 + \frac{\mu_2 - \mu_1}{1 + I_0/I}}_{\mu^{cont}} + \underbrace{I + \frac{5}{2}C_{max}I^{1/2}}_{\mu^{hydro}}, \quad C_p(I) = \frac{C_{max}}{1 + I^{1/2}}$$

Here $\mu_1 = 0.32$, $\mu_2 = 0.7$, $I_0 = 0.005$, and $C_{max} = 0.585$. The work [129] proposed an improvement for this relation in the form:

$$\mu^{cont} = \mu_1 + \frac{C_{max} - C}{\beta}$$

with $\mu_1 = 0.3$, $\beta = 0.158$ being the 'compressibility' factor, and $C_{max} = 0.585$, demonstrating a better match with experiments and adequate behavior in dilute and packing limits. The total expression for rheology is given by [129]:

$$\mu_s(C_p) = \underbrace{\mu_1 + \frac{C_{max}}{\beta} \left(1 - \frac{C_p}{C_{max}}\right)}_{\mu^{cont}} + \underbrace{\left(I + \left(\frac{5}{2}C_{max} + 2\right)I^{1/2}\right)}_{\mu^{hydro}}$$

$$I(C_p < C_{max}) = \left(\frac{C_{max}}{C_p} - 1\right)^2, \text{ and } I(C_p \geq C_{max}) = 0$$

Both models [34] and [129] were discussed in comparison with magnetic resonance imaging of suspensions in [130]. This approach to unifying the rheology of suspension between the flowing suspension and the closely packed granular medium appears to be most promising, and it will be quite interesting to see what it yields once implemented in a global 2D modeling framework for proppant transport and settling on the fracture scale. The generalization of this rheology model to the case of a non-Newtonian carrier fluid is still in progress [46].

If the proppant concentration at any point in the fracture reaches the maximum packing limit, it is proposed [80] that fluid flow can be simulated as flow through a porous medium, using Darcys law with a certain correlation for the permeability K_p of the proppant pack:

$$\mathbf{v} = -\frac{K_p}{\mu_f} \nabla p, \quad K_p = K_k a^2 f(\phi),$$

The value of K_p is, in general, a function of the mean proppant grain size a (also understood as the radius of equivalent sphere having the same volume) and the pack porosity ϕ . Here K_k is an empirical constant. Pore-scale simulations combined with conductivity tests in the lab indicate the following empirical relation valid for spatially periodical random close packings of spherical and elongated particles (ellipsoids, cylinders) in a wide range of porosity ($0.3 < \phi < 0.7$) [154]:

$$K_p = 0.204a^2\phi^{4.58}$$

Sometimes K_p is set for simplicity as a constant value, which approximately corresponds to loose sand. One of the approaches could be to establish a smooth and gradual transition between the conductivity of the open fracture ($w^2/12$) and the permeability of the proppant K_p , which would remove the singularity in the pressure equation 8 due to jumps in the conductivity maps. Though, generally there are stable schemes for displacements with high contract in viscosity [31]. It will be of particular interest to implement the unified granular rheology model [34, 129] (spanning from dilute suspension to packing limit) into a global 2D proppant transport modeling framework in order to provide a monotonic and continuous transition from flowing suspension to packed bed.

Fluid leakoff from packed elements is another issue. Some of the assumptions behind Carter's leakoff model break down in this case: e.g., filter cake is no longer a thin layer building only on the fracture walls. The fluid pressure inside the packed elements decreases due to the low conductivity to the point where the pressure drop between the fracture and the reservoir is no longer large. Furthermore, the fact that Carter's law is not dependent on the proppant concentration does not allow for a gradual transition of the leak-off from pure liquid to close packing. As a trade-off, some models relate the permeability of the packed domain with the conductivity of an open fracture via some reduction coefficient (say, 0.2). Again, this is a part of the model that requires further improvement.

Bridging. Bridging or arching are caused by geometric constraints. In a pressure driven flow of suspension through a narrow channel with rough walls, interactions between particles and with the walls result in particles lagging behind the flow and slowing down, which will eventually result in the increase of the mean particle volume fraction. When the fracture width gets small enough for the bridging criteria to be met (see below for particular closure relations for the bridging criterion), this process eventually leads to the concentration reaching maximum packing limit. At some stage, however, it is also possible that even before reaching C_{max} , the particles may literally become lodged between the slot faces. Because the particles do not re-arrange in the form of a regular train along the fracture, they get locked across the slot, forming a "bridge" or an "arch" between the faces. This bridge is usually kept in place by the contact stresses (transmitted from face to face through the particles), the roughness of the particles, and embedment of the particles into the fracture faces. Once a bridge is formed, it usually results in the arrest of the suspension transport upstream this point. The most commonly used model for bridging consists of defining a certain threshold width, at which the particles

form a bridge or an arch. If in any part of the fracture the width is equal or less than this critical width w^* , the proppant should not be allowed to flow through it. The work [211] determined experimentally the bridging factor $b = w^*/d = 2.6$, which is the criterion currently used by some commercial simulators by default. For low proppant loading, the bridging factor was found to be 1.8. In the industry, it has become customary to use this simplified criterion of bridging in terms of the bridging factor taken as a constant from the interval $w^*/d \in [2.5 - 3]$ [81, 52].

More sophisticated criteria take into account experimental observations [78], which demonstrate that the critical width is also dependent upon the concentration of proppant upstream of the bridging point. Although the original criterion of [78] was developed for modeling bridging at perforations, the work [112] reported a modified version for bridging in a fracture, which demonstrate

$$w^* = \min \left[b, 1 + \frac{C_p}{0.17}(b-1) \right] d$$

where the bridging factor $b = 2.5$ by default, d is the particle diameter, and C_p is the particle volume fraction in flowing suspension.

The effects of fibers on bridging have been studied in [207, 208] based on the partitioning of energy approach following Bagnold's theory. Flow energy imparted to the moving slurry is partitioned into useful shear work, kinetic energy of particles, and a portion lost in dissipative solid-body interactions. A modified bridging criterion was proposed in the form $B_{cr} \sim T_{EP}T_B T_{FC}$, where T_i are energy spent for energy partitioning, blockage, and particle-fibers interactions, respectively. Closures for T_i were expressed via volume fraction of fibers C_f based on phenomenological considerations, though we think fibers crowding parameter $N = (2/3)C_f(l_f/d_f)^2$ [134] is a better measure of fibers impact than pure fibers volume concentration. A recent experimental study of bridging in slots with tapered walls can be found in [166], where the key finding was that for slots with smooth walls $b = w^*/d \approx 1$.

On the fracture scale, bridging and packing in application to tip screenout (TSO) was studied in [41, 51, 53]. The work [41] split the entire fracture into the flowing suspension region $C_p < C_{max}$ and the porous medium of packed proppant $C_p = C_{max}$, where the Darcy law applies. KGD model was used for fracture propagation, and a more complex than Carter's relation was used for leak-off. In turn, the works of [51, 53] utilized frictional rheology of [34] to study 3D slurry flow in a fracture and transition to packing, also including transition to Darcy's flow in packed region. Detailed comparison with concurrent works of [129] are given. For proppant flowback, see Sec. 4.1.

6. Conclusions and Future Directions

Multiphase fluid mechanics of hydraulic fracturing is critically reviewed via comparison of the state of the art in modeling with the recent advancements in technology now used routinely in the field. Technology moves forward. Not because of predictive modeling, but thanks to empirical trial-and-error in massive

field testing. Modeling is lagging behind the technology by a period of more than 10 years. To bridge this gap, it is proposed to have a systematic view and structure research by geometry and flow regime: (i) high-Re 1D flows during proppant transport down the well, (ii) low-inertia 2D creeping flows in fractures, and (iii) multiscale flowback after the stimulation, which couples 3D flow in the reservoir, 2D flow in fracture network, and highly-transient 1D gas-liquid flow in the near-horizontal well. Let us put forward that the modelling of proppant placement and flowback in hydraulic fractures is as good as its closure relations. In finding the closures, experimental support is of undoubted importance.

With progress in contemporary fracturing technology, standard rheometry is no longer applicable to mixtures of visco-elasto-plastic fluid, particles, and fibers, which requires novel methods in experimentation. Fracturing fluids are everything but Newtonian, and a fiber-laden slurry is sometimes everything but fluid when close to the packing limit, where all existing suspension viscosity models diverge. Yield stress, visco-elasticity of fracturing fluids, fibers, dune transport are not systematically included into fracturing simulators, despite such systems have been used routinely in the field for at least a decade. Semi-empirical kinematic conditions for proppant bridging and proppant flowback need to be replaced with dynamic conditions based on coupled solid-fluid mechanics considerations. In shales, Carter's leak-off and Darcy law are no longer valid, which calls for models of fluid outflow into natural fractures and imbibition into the matrix.

Equally important is to properly model the flowback from a fractured well, as the value created during the stimulation treatment may be quickly lost due to excessive drawdown when flowing back a well at too high rates, leading to undesired geomechanics events and eventually hydraulic disconnection of the fracture from the well. The same is true for the practice of overflushing in unconventional, when excessive displacement of the treatment slurry into the fracture may result in a pinch-out. Unlike pumping the stimulation treatment, when the steady-state wellbore hydraulic is, in fact, decoupled from proppant placement in fractures, flowback is essentially a coupled phenomenon, where pressure oscillations due to slug flow in the near-horizontal well have impact on both fluid flow and geomechanics in the propped fracture.

We said above that modeling of proppant transport is all about the constitutive relationships. But the global modeling framework is also important. Effective-medium models for suspension should be updated within two-fluid approach to include two-speed effects due to inter-phase slip. Traditional lubrication approximation fails to capture real fracture morphology in shales, as well as Darcy law is no longer suitable for modeling of leak-off into, and flowback from, ultra-low permeability matrix in unconventional. Avenues to enhance the model by including elements of real fracture geometry are proposed.

On the final note, given the complexity of the discipline of proppant placement and flowback in wells and fractures, modeling needs to be developed tightly linked with, and supported by, systematic lab experiments, both for selection of constitutive relationships and for validation of the results for proppant

placement patterns. Probation of the resulting treatment design on real field data is required.

7. Acknowledgments

The author is greatly indebted to Jean Desroches for a detailed review of this paper and many constructive remarks, which helped a lot to improve the final version of this manuscript; the author is also grateful to his former colleagues at Schlumberger R&D for continuous discussions on the topic of this paper over the past 10 years, which helped build a broader view on applied aspects of relevant fundamental problems. Particularly insightful discussions with J.R.A. Pearson and P.S. Hammond are highly appreciated.

Start-up funds provided by Skolkovo Institute of Science and Technology (Skoltech) are gratefully acknowledged.

8. Disclaimer

When working on this paper, the author was not affiliated with, or funded by, any vendor of commercial fracture simulation software, which might be perceived as affecting the objectivity of this review.

Index	Definition
<i>c</i>	Related to the channel
<i>L</i>	Related to leak-off
<i>p</i>	Related to particles
<i>s</i>	Related to sedimentation
<i>sl</i>	Related to slurry
<i>St</i>	Governed by the Stokes law (settling)
<i>T</i>	Related to thixotropy

Table 8: Nomenclature: indexes and their definitions.

- [1] Acharya, A.R., 1986. Particle transport in viscous and viscoelastic fracturing fluids. *SPE Production Engineering*, 1(02), pp.104-110.
- [2] Acrivos, A. & Herbolzheimer, E. 1979 Enhanced sedimentation in settling tanks with inclined walls. *J. Fluid Mech.* **92**, 435-457.
- [3] Davis, R.H. and Acrivos, A., 1985. Sedimentation of noncolloidal particles at low Reynolds numbers. *Annual Review of Fluid Mechanics*, 17(1), pp.91-118.
- [4] Leighton, D. and Acrivos, A., 1987. The shear-induced migration of particles in concentrated suspensions. *Journal of Fluid Mechanics*, **181**, 415-439.
- [5] Aksakov, A.V., Borshchuk, O.S., et al. 2016. Corporate fracturing simulator: from a mathematical model to the software development, *Oil Industry*, 11, 35-40.
- [6] Asgian, M.I., Cundall, P.A. and Brady, B.H.G., 1995. The mechanical stability of propped hydraulic fractures: a numerical study. *Journal of Petroleum Technology*, 47(03), pp.203-208. Vancouver.
- [7] Asmolov, E.S., 1999. The inertial lift on a spherical particle in a plane Poiseuille flow at large channel Reynolds number. *Journal of Fluid Mechanics*, 381, pp.63-87.
- [8] Asmolov, E.S., 1990. Dynamics of a spherical particle in a laminar boundary layer. *Fluid Dynamics*, 25(6), pp.886-890.
- [9] Asmolov, E.S. & Osipov, A.A. 2009 The inertial lift on a spherical particle settling in a horizontal viscous flow through a vertical slot. *Phys. Fluids* **21**, 063301.
- [10] Ayoub, J.A., Hutchins, R.D., Van der Bas, F., Cobianco, S., Emilian, C.N., Glover, M.D., Marino, S., Nitters, G., Norman, D. and Turk, G.A., 2006, January. New results improve fracture cleanup characterization and damage mitigation. In SPE Annual Technical Conference and Exhibition. Society of Petroleum Engineers.

- [11] Bagnold, R.A., 2012. The physics of blown sand and desert dunes. Courier Corporation.
- [12] Bagnold, R.A., 1973, April. The nature of saltation and of bed-load transport in water. In Proceedings of the Royal Society of London A: Mathematical, Physical and Engineering Sciences (Vol. 332, No. 1591, pp. 473-504). The Royal Society.
- [13] Balhoff, M. and Miller, M.J., 2002, January. Modeling Fracture Fluid Cleanup in Hydraulic Fractures. In SPE Annual Technical Conference and Exhibition. Society of Petroleum Engineers.
- [14] Balhoff, M.T. and Miller, M.J., 2005. An analytical model for cleanup of yield-stress fluids in hydraulic fractures. *SPE journal*, 10(01), pp.5-12.
- [15] Barree, R.D. and Conway, M.W., 1994, January. Experimental and numerical modeling of convective proppant transport. In SPE Annual Technical Conference and Exhibition. Society of Petroleum Engineers.
- [16] Barree, R.D. and Mukherjee, H., 1996, January. Determination of pressure dependent leakoff and its effect on fracture geometry. In SPE Annual Technical Conference and Exhibition. Society of Petroleum Engineers.
- [17] Bautista, F., Soltero, J.F.A., Prez-Lpez, J.H., Puig, J.E. and Manero, O., 2000 On the shear banding flow of elongated micellar solutions. *Journal of Non-Newtonian Fluid Mechanics*, **94**(1), 57-66.
- [18] Adachi, J., Siebrits, E., Peirce, A., & J. Desroches, 2007 Computer simulation of hydraulic fractures. *Int. J. of Rock Mech. and Mining Sci.* **44** (1), 739757.
- [19] Bai, M., Green, S. and Suarez-Rivera, R., 2005, January. Effect of leakoff variation on fracturing efficiency for tight shale gas reservoirs. In Alaska Rocks 2005, the 40th US Symposium on Rock Mechanics (USRMS). American Rock Mechanics Association.
- [20] Barbati, A. C., Desroches, J., Robisson, A., & McKinley, G. H. 2016 Complex Fluids and Hydraulic Fracturing. *Annual review of chemical and biomolecular engineering*, **7**, 415-453.
- [21] Barree, R.D., 1983, January. A practical numerical simulator for three-dimensional fracture propagation in heterogeneous media. In SPE Reservoir Simulation Symposium. Society of Petroleum Engineers. Paper SPE 12273.
- [22] Batchelor, G.K., 1972. Sedimentation in a dilute dispersion of spheres. *Journal of fluid mechanics*, 52(02), pp.245-268.
- [23] G.K. Batchelor, 1977 The effect of Brownian motion on bulk stress in a suspension of spherical particles, *J. Fluid Mech.* **83**, 97- 117.
- [24] Bendiksen, K.H., Maines, D., Moe, R. and Nuland, S., 1991. The dynamic two-fluid model OLGA: Theory and application. *SPE production engineering*, 6(02), pp.171-180.
- [25] Bochkarev, A., Budennyy, S., Nikitin, R. and Mitrushkin, D., 2016, August. Pseudo-3D Hydraulic Fracture Model with Complex Mechanism of Proppant Transport and Tip Screen Out. In ECMOR XV-15th European Conference on the Mathematics of Oil Recovery.
- [26] Bochkarev A.V., Budennyy S.A., Nikitin R.N., Mitrushkin D.A., Erofeev A.A., Zhukov V.V. 2017. Optimization of multi-stage hydraulic fracturing design in conditions of Bazhenov formation, Oil Industry. N3. pp. 50-53.
- [27] Boek, E.S., Hall, C., Tardy, P.M.J. Deep Bed Filtration Modelling of Formation Damage due to Particulate Invasion from Drilling Fluids, Transport in Porous Media, V. 91-2, pp. 479508, 2012.
- [28] Boronin, S. A., & Osipov, A. A. 2010 Two Continua Model of Suspension Flow in a Hydraulic Fracture. *Doklady Physics*. **55**(4), 192–202.
- [29] Boronin, S.A. & Osipov, A.A., 2014. Effects of particle migration on suspension flow in a hydraulic fracture. *Fluid Dynamics*, **49**(2), 208-221.
- [30] Boronin, S.A., Osipov, A.A. and Tolmacheva, K.I., 2015. Multi-fluid model of suspension filtration in a porous medium. *Fluid Dynamics*, **50**(6), pp.759-768.
- [31] Boronin, S.A., Osipov, A.A., & Desroches, J. 2015. Displacement of yield-stress fluids in a fracture , *Int. J. Multiphase Flow*, **76**, 4763.
- [32] Boronin, S.A., Private communication. 2017.
- [33] Boronin, S.A., Osipov, A.A. 2017. Multigrid pressure solver for proppant transport modeling in hydraulic fracturing simulators, In Proceedings of the Third EAGE Workshop High Performance Computing for Upstream, 1-4 October 2017, Athens, Greece. pp. 1-4 (accepted, to appear).
- [34] Boyer, F., Guazzelli, . and Pouliquen, O., 2011. Unifying suspension and granular rheology. *Physical Review Letters*, 107(18), p.188301.
- [35] Bratland, O., 2010. Pipe Flow 2: Multi-phase Flow Assurance. *Ove Bratland*.
- [36] Brown S. R., 1987. Fluid flow through rock joints: the effect of surface roughness, *Journal of Geophysical Research: Solid Earth*. **92**(B2), 1337-1347.
- [37] Burukhin, A.A., Kalinin, S., Abbott, J., Bulova, M., Wu, Y.K., Crandall, M., Kadoma, I., Begich, M. and Papp, S., 2012, January. Novel interconnected bonded structure enhances proppant flowback control. In SPE International Symposium and Exhibition on Formation Damage Control. Society of Petroleum Engineers.
- [38] Carter, R.D.: Derivation of the General Equation for Estimating the Extent of the Fractured Area, Appendix I of Optimum Fluid Characteristics for Fracture Extension, Drilling and Production Practice, G.C. Howard and C.R. Fast, New York, New York, USA, American Petroleum Institute (1957), 261269.
- [39] Cassar, C., Nicolas, M. and Pouliquen, O., 2005. Submarine granular flows down inclined planes. *Physics of Fluids* (1994-present), **17**(10), p.103301.
- [40] Chateau, X., Ovarlez, G. and Trung, K.L., 2008. Homogenization approach to the behavior of suspensions of noncolloidal particles in yield stress fluids. *Journal of Rheology*, **52**(2), pp.489-506.
- [41] Chekhanin, E. and Levonyan, K., 2012. Hydraulic fracture propagation in highly permeable formations, with applications to tip screenout. *International Journal of Rock Mechanics and Mining Sciences*, **50**, pp.19-28.
- [42] Civan, F., Reservoir Formation Damage. Fundamentals, Modeling, Assessment, and Mitigation. Second edition. - Gulf Professional Publishing, Oxford, USA, 1135 pages. 2007.
- [43] Clifton, R.J. and Wang, J.J., 1988, January. Multiple fluids, proppant transport, and thermal effects in three-dimensional simulation of hydraulic fracturing. In SPE Annual Technical Conference and Exhibition. Society of Petroleum Engineers.
- [44] Cox R. G., Brenner H. 1968 The lateral migration of solid particles in Poiseuille flow. I. Theory. *Chem. Eng. Sci.* **23**, 147173.
- [45] Cox, R.G. and Hsu, S.K., 1977. The lateral migration of solid particles in a laminar flow near a plane. *International Journal of Multiphase Flow*, **3**(3), pp.201-222.
- [46] Dagois-Bohy, S., Hormozi, S., Guazzelli, . and Pouliquen, O., 2015. Rheology of dense suspensions of non-colloidal spheres in yield-stress fluids. *Journal of Fluid Mechanics*, 776.
- [47] Danielson, T.J., Bansal, K.M., Djoric, B., Larrey, D., Johansen, S.T., De Leebeck, A. and Kjolaas, J., 2012, April. Simulation of slug flow in oil and gas pipelines using a new transient simulator. In Offshore Technology Conference. Offshore Technology Conference.
- [48] De Henau, V. and Raithby, G.D., 1995. A study of terrain-induced slugging in two-phase flow pipelines. *International journal of multiphase flow*, **21**(3), pp.365-379.
- [49] Detournay, E., 2016. Mechanics of hydraulic fractures. *Annual Review of Fluid Mechanics*, **48**, pp.311-339.
- [50] Dogon, D. and Golombok, M., 2016. Wellbore to fracture proppant-placement-fluid rheology. *Journal of Unconventional Oil and Gas Resources*, **14**, pp.12-21.
- [51] Dontsov, E.V. and Peirce, A.P., 2014. Slurry flow, gravitational settling and a proppant transport model for hydraulic fractures. *Journal of Fluid Mechanics*, **760**, pp.567-590.
- [52] Dontsov, E.V. and Peirce, A.P., 2014. A new technique for proppant schedule design. *Hydraul Fract J*, **1**(3).
- [53] Dontsov, E.V. and Peirce, A.P., 2015. Proppant transport in hydraulic fracturing: Crack tip screen-out in KGD and P3D models. *International Journal of Solids and Structures*, **63**, pp.206-218.
- [54] Doron, P., Granica, D. and Barnea, D., 1987. Slurry flow in horizontal pipesexperimental and modeling. *International Journal of Multiphase Flow*, **13**(4), pp.535-547.
- [55] Doron, P. and Barnea, D., 1993. A three-layer model for solid-liquid flow in horizontal pipes. *International Journal of Multiphase Flow*, **19**(6), pp.1029-1043.
- [56] Doron, P. and Barnea, D., 1996. Flow pattern maps for solid-liquid flow in pipes. *International journal of multiphase flow*, **22**(2), pp.273-283.
- [57] Economides, M.J. & Nolte, K.G. *Reservoir Stimulation*. Third Edition. Wiley, 2000.
- [58] A. Einstein, 1906 A new method of determining molecular dimensions, *Annu. Phys.* **19**, 289-306.
- [59] Engels, J.N., Martinez, E., Fredd, C.N., Boney, C.L., Holmes, B.A., 2004. A Mechanical Methodology of Improved Proppant Transport in Lowviscosity Fluids: Application of a Fiber-assisted Transport Technique in East Texas. SPE91434.

- [60] Eskin, D., Leonenko, Y., Vinogradov, O. 2004 On a turbulence model for slurry flow in pipelines. *Chem. Eng. Sci.* **59**, 557-565,
- [61] Eskin, D. 2005 An engineering model of solids diffusivity in hydraulic conveying. *Powder Technology*, **159**, 78-86.
- [62] Eskin, D. and Miller, M.J., 2008. A model of non-Newtonian slurry flow in a fracture. *Powder Technology*, **182**(2), 313-322.
- [63] Eskin, D. A simple model of particle diffusivity in horizontal hydrotransport pipelines. 2012 *Chem. Eng. Sc.*, **82**, pp. 8494.
- [64] Evje, S. and Fjelde, K.K., 2002. Hybrid flux-splitting schemes for a two-phase flow model. *Journal of Computational Physics*, 175(2), pp.674-701.
- [65] Munkejord, S.T., Evje, S. and Flitten, T., 2006. The multistage centred-scheme approach applied to a driftflux twophase flow model. *International Journal for Numerical Methods in Fluids*, 52(6), pp.679-705.
- [66] Evje, S. and Flitten, T., 2007. On the wave structure of two-phase flow models. *SIAM Journal on Applied Mathematics*, 67(2), pp.487-511.
- [67] Frankel, N.A. and Acrivos, A., 1967. On the viscosity of a concentrated suspension of solid spheres. *Chemical Engineering Science*, 22(6), pp.847-853.
- [68] F. Ferrini, D. Ercolani, B.D. Cindio, L. Nicodemo, L. Nicolais, S. Ranaudo, 1979 Shear viscosity of settling suspensions, *Rheol. Acta*, **18** (2), 289-296.
- [69] Bivins, C.H., Boney, C., Fredd, C., Lassek, J., Sullivan, P., Engels, J., Fielder, E.O., Gorham, T., Judd, T., Mogollon, A.E.S. and Tabor, L., 2002. New fibers for hydraulic fracturing. *Science*, 83(2), pp.660-686.
- [70] Crockett, A.R., Okusu, N.M. and Cleary, M.P., 1986, January. A complete integrated model for design and real-time analysis of hydraulic fracturing operations. In SPE California Regional Meeting. Society of Petroleum Engineers. Paper SPE 15069.
- [71] Cleary, M.P., Barr, D.T. and Willis, R.M., 1988, January. Enhancement of real-time hydraulic fracturing models with full 3-D simulation. In SPE Gas Technology Symposium. Society of Petroleum Engineers. Paper SPE 17713.
- [72] Gadala-Maria F, Acrivos A. 1980. Shearinduced structure in a concentrated suspension of solid spheres. *J. Rheol.* **24**(6) 799814
- [73] Garagash, I.A. 2010. Numerical modeling of a hydraulic fracture in dilatant weak rocks and evolution of proppant porosity, *In Book of Abstracts: 10th Hydraulic Fracturing Summit*, 15-18 July 2010, Limassol, Cyprus.
- [74] Gauthier, F., Goldsmith, H.L. and Mason, S.G., 1971. Particle Motions in NonNewtonian Media. II. Poiseuille Flow. *Transactions of the Society of Rheology*, 15(2), pp.297-330.
- [75] Gidaspow, D., 1994. Multiphase flow and fluidization: continuum and kinetic theory descriptions. Academic press.
- [76] Gillard, M.R., Medvedev, O.O., Hosein, P.R., Medvedev, A., Pe nacorada, F., Huteau, E., 2010. A New Approach to Generating Fracture Conductivity. SPE 135034.
- [77] Goel, N. and Shah, S.N., 1999, January. Experimental investigation of proppant flowback phenomena using a large scale fracturing simulator. In SPE Annual Technical Conference and Exhibition. Society of Petroleum Engineers.
- [78] Gruesbeck, C. and Collins, R.E., 1982. Particle transport through perforations. *Society of Petroleum Engineers Journal*, 22(06), pp.857-865.
- [79] Garside, J. and Al-Dibouni, M.R., 1977. Velocity-voidage relationships for fluidization and sedimentation in solid-liquid systems. *Industrial & engineering chemistry process design and development*, 16(2), pp.206-214.
- [80] Gu, H. & Siebrits, E. 2004 On the numerical solution of hyperbolic proppant transport problems. *In: Proceedings of the 10-th international conference on hyperbolic problems: theory, numerics and applications, Osaka, Japan, September 1317, 2004.*
- [81] Gu, H. and Desroches, J., 2003, January. New pump schedule generator for hydraulic fracturing treatment design. In SPE Latin American and Caribbean petroleum engineering conference. Society of Petroleum Engineers.
- [82] Guazzelli, . and Hinch, J., 2011. Fluctuations and instability in sedimentation. *Annual review of fluid mechanics*, 43, pp.97-116.
- [83] Guo, J., Ma, J., Zhao, Z. and Gao, Y., 2015. Effect of fiber on the rheological property of fracturing fluid. *Journal of Natural Gas Science and Engineering*, 23, pp.356-362.
- [84] Hawksley, P.G.W., 1951. The effect of concentration on the settling of suspensions and flow through porous media. Some aspects of fluid flow, pp.114-135.
- [85] Hammond, P. S. 1995 Settling and slumping in a Newtonian slurry, and implications for proppant placement during hydraulic fracturing of gas wells, *Chem. Eng. Sci.* **50** (20), 3247.
- [86] Herzig J. P., Leclerc D. M., Goff P. L. Flow of suspensions through porous media application to deep filtration, *Industrial and Engineering Chemistry* V.625, pp. 8-35, 1970.
- [87] Herzhaft, B., Guazzelli, ., Mackaplow, M.B. and Shaqfeh, E.S., 1996. Experimental investigation of the sedimentation of a dilute fiber suspension. *Physical review letters*, 77(2), p.290.
- [88] Ho, B.P. and Leal, L.G., 1974. Inertial migration of rigid spheres in two-dimensional unidirectional flows. *Journal of fluid mechanics*, 65(02), pp.365-400.
- [89] Ho, B.P. and Leal, L.G., 1976. Migration of rigid spheres in a two-dimensional unidirectional shear flow of a second-order fluid. *Journal of Fluid Mechanics*, 76(04), pp.783-799.
- [90] Hogg, A.J., 1994. The inertial migration of non-neutrally buoyant spherical particles in two-dimensional shear flows. *Journal of Fluid Mechanics*, 272, pp.285-318.
- [91] Hormozi, S. 2013 Transport and dispersion of particles in visco-plastic fluids, MSc thesis, The University of British Columbia.
- [92] Hormozi, S. & Frigaard, I., 2016 Dispersion of solids in fracturing flows of yield stress fluids. *Bulletin of the American Physical Society*, 61.
- [93] Hormozi, S., and Frigaard, I.A. 2017 Dispersion of solids in fracturing flows of yield stress fluids. *J. Fluid Mech. (under review)*.
- [94] Howard GC, Fast CR. 1970. Hydraulic Fracturing, Vol. 2, Monograph (Society of Petroleum Engineers of AIME), Henry L. Doherty Series. New York: Soc. Pet. Eng.
- [95] Schonberg, J.A. and Hinch, E.J., 1989. Inertial migration of a sphere in Poiseuille flow. *Journal of Fluid Mechanics*, 203, pp.517-524.
- [96] Patankar, N.A., Huang, P.Y., Ko, T. and Joseph, D.D., 2001. Lift-off of a single particle in Newtonian and viscoelastic fluids by direct numerical simulation. *Journal of Fluid Mechanics*, 438, pp.67-100.
- [97] Issa, R.I. and Kempf, M.H.W., 2003. Simulation of slug flow in horizontal and nearly horizontal pipes with the two-fluid model. *International journal of multiphase flow*, 29(1), pp.69-95.
- [98] Kadri, U., Mudde, R.F., Oliemans, R.V.A., Bonizzi, M. and Andreussi, P., 2009. Prediction of the transition from stratified to slug flow or roll-waves in gasliquid horizontal pipes. *International Journal of Multiphase Flow*, 35(11), pp.1001-1010.
- [99] Karnis, A. and Mason, S.G., 1966. Particle motions in sheared suspensions. XIX. Viscoelastic media. *Transactions of the Society of Rheology*, 10(2), pp.571-592.
- [100] Kern, L.R., T.K. Perkins, and R.E. Wyant. 1959. The mechanics of sand movement in fracturing. *JPT*. July 1959. pp. 55-57.
- [101] Klinkenberg LJ. 1941. The permeability of porous media to liquids and gases. Presented at Drill. Pract., Jan. 1, New York.
- [102] I.M. Krieger, T.J. Dougherty, 1959 A mechanism for non-Newtonian flow in suspensions of rigid spheres, *Trans. Soc. Rheol.*, **3**, 137152.
- [103] I.M. Krieger, 1972 Rheology of monodisperse latices, *Adv. Colloid Interface Sci.*, **3**, 111-136.
- [104] Kuchuk, F.J., Goode, P.A., Brice, B.W., Sherrard, D.W. and Thambynayagam, R.K., 1990. Pressure-transient analysis for horizontal wells. *Journal of Petroleum Technology*, 42(08), pp.974-1.
- [105] Kuchuk, F.J., Onur, M. and Hollaender, F., 2010. Pressure transient formation and well testing: convolution, deconvolution and nonlinear estimation (Vol. 57). Elsevier.
- [106] Kuchuk, F. and Biryukov, D., 2015. Pressure-transient tests and flow regimes in fractured reservoirs. *SPE Reservoir Evaluation & Engineering*, 18(02), pp.187-204.
- [107] Landel, RF, BG Moser and A. Bauman, Rheology of Concentrated Suspensions: Effect of a Surfactant, Proceeding of the Fourth International Congress of Rheology, Providence, Rhode Island, USA, 1963(Pt. 2), 663-692 (1965)
- [108] Larson, R.G., 1999. The structure and rheology of complex fluids (Vol. 150). New York: Oxford university press.
- [109] Asmolov, E. S., Lebedeva, N. A., & Osipov, A. A. 2009 Inertial Migration of Sedimenting Particles in a Suspension Flow through a HeleShaw Cell. *Fluid Dynamics*, **44** (3), 405418.
- [110] Liapidevskii, V.Y. and Tikhonov, V., 2016, June. Lagrangian approach to modeling unsteady gas-liquid flow in a well. In *Journal of Physics: Conference Series* (Vol. 722, No. 1, p. 012026). IOP Publishing.

- [111] Liapidevskii, V.Y. and Tikhonov, V.S., 2017, February. Modulation equations for slug flow in vertical pipes. In Doklady Physics (Vol. 62, No. 2, pp. 80-84). Pleiades Publishing.
- [112] Mack, M.G. and Warpinski, N.R., 2000. Mechanics of Hydraulic Fracturing. In Economides M.J. and Nolte, K.G. (eds.), Reservoir Stimulation, Chichester: Wiley.
- [113] Mahaut, F., Chateau, X., Coussot, P. and Ovarlez, G., 2008. Yield stress and elastic modulus of suspensions of noncolloidal particles in yield stress fluids. *Journal of Rheology*, 52(1), pp.287-313.
- [114] Matas, J.P., Morris, J.F. and Guazzelli, ., 2004. Inertial migration of rigid spherical particles in Poiseuille flow. *Journal of Fluid Mechanics*, 515, pp.171-195.
- [115] Matas, J.P., Morris, J.F. and Guazzelli, E., 2004. Lateral forces on a sphere. *Oil & gas science and technology*, 59(1), pp.59-70.
- [116] Matas, J.P., Morris, J.F. and Guazzelli, E., 2009. Lateral force on a rigid sphere in large-inertia laminar pipe flow. *Journal of Fluid Mechanics*, 621, pp.59-67.
- [117] McLennan, J.D., Green, S.J. and Bai, M., 2008, January. Proppant placement during tight gas shale stimulation: literature review and speculation. In The 42nd US Rock Mechanics Symposium (USRMS). American Rock Mechanics Association.
- [118] McLennan, J., Walton, I., Moore, J., Brinton, D. and Lund, J., 2015. Proppant backflow: Mechanical and flow considerations. *Geothermics*, 57, pp.224-237.
- [119] Meyer, B.R., 1989. Three-Dimensional Hydraulic Fracturing Simulation on Personal Computers: Theory and Comparison Studies, paper SPE 19329, Oct.,1989.
- [120] Meyer, B.R., Cooper, G.D. and Nelson, S.G., 1990, January. Real-time 3-D hydraulic fracturing simulation: theory and field case studies. In SPE Annual Technical Conference and Exhibition. Society of Petroleum Engineers. Paper SPE 20658.
- [121] Miller, M.J., Schlumberger Technology Corporation, 2013. Well Treatment. U.S. Patent Application 14/016,571.
- [122] McLaughlin, J. B. 1991 Inertial migration of a small sphere in linear shear ows. *J. Fluid Mech.* 224: 261274.
- [123] McLaughlin, J.B., 1993. The lift on a small sphere in wall-bounded linear shear flows. *Journal of Fluid Mechanics*, 246, pp.249-265.
- [124] McClure, M.W. and Kang, C.A., 2017, February. A Three-Dimensional Reservoir, Wellbore, and Hydraulic Fracturing Simulator that is Compositional and Thermal, Tracks Proppant and Water Solute Transport, Includes Non-Darcy and Non-Newtonian Flow, and Handles Fracture Closure. In SPE Reservoir Simulation Conference. Society of Petroleum Engineers.
- [125] Milton-Taylor, D., Stephenson, C. and Asgian, M.I., 1992, January. Factors affecting the stability of proppant in propped fractures: results of a laboratory study. In SPE Annual Technical Conference and Exhibition. Society of Petroleum Engineers.
- [126] Morris, J.P., Schlumberger Technology Corporation, 2014. Method for performing a stimulation operation with proppant placement at a wellsite. U.S. Patent Application 14/460,654.
- [127] Morris, J.P., Chochua, G.G. and Bogdan, A.V., 2015. An efficient non-newtonian fluidflow simulator for variable aperture fractures. *The Canadian Journal of Chemical Engineering*, 93(11), pp.1902-1915.
- [128] P.R. Nott, J.F. Brady, 1994 Pressure-driven flow of suspensions: simulation and theory. *J. Fluid Mech.* 275, 157-159.
- [129] Lecampion, B. and Garagash, D.I., 2014. Confined flow of suspensions modelled by a frictional rheology. *Journal of Fluid Mechanics*, 759, 197-235.
- [130] Oh, S., Song, Y.Q., Garagash, D.I., Lecampion, B. and Desroches, J., 2015. Pressure-driven suspension flow near jamming. *Physical review letters*, 114 (8), p.088301.
- [131] Lebedeva, N.A. & Asmolov, E.S. 2011 Migration of settling particles in a horizontal viscous flow through a vertical slot with porous walls. *Int. J. of Multiphase Flow*. 37 (5), 453461.
- [132] Lhuillier, D., 2009. Migration of rigid particles in non-Brownian viscous suspensions. *Physics of Fluids*, 21(2), p.023302.
- [133] Liu, Y. and Sharma, M.M., 2005, January. Effect of fracture width and fluid rheology on proppant settling and retardation: an experimental study. In SPE annual technical conference and exhibition. Society of Petroleum Engineers.
- [134] Lundell, F., Sderberg, L.D. and Alfredsson, P.H., 2011. Fluid mechanics of papermaking. *Annual Review of Fluid Mechanics*, 43, pp.195-217.
- [135] M. Mack and N. Warpinski, Mechanics of Hydraulic Fracturing, in Reservoir Stimulation 3rd Edition, Editors M.J. Economides and K.G. Nolte, John Wiley and Sons, West Sussex U.K., pp. 6-1, 6-49. 2000
- [136] Mack, M., Sun, J., & Khadilkar, C. 2014. Quantifying proppant transport in thin fluids: theory and experiments. In SPE Hydraulic Fracturing Technology Conference. Society of Petroleum Engineers.
- [137] Maron, S.H. and Pierce, P.E., 1956. Application of Ree-Eyring generalized flow theory to suspensions of spherical particles. *Journal of colloid science*, 11(1),80-95.
- [138] Matas, J.P., Glezer, V., Guazzelli, . and Morris, J.F., 2004. Trains of particles in finite-Reynolds-number pipe flow. *Physics of Fluids*, 16(11), pp.4192-4195.
- [139] Metzger, B., Nicolas, M. and Guazzelli, ., 2007. Falling clouds of particles in viscous fluids. *Journal of Fluid Mechanics*, 580, pp.283-301.
- [140] Neto, L.B. and Kotousov, A., 2013. On the residual opening of hydraulic fractures. *International Journal of Fracture*, 181(1), pp.127-137.
- [141] Nicodemo, L., Nicolais, L. and Landel, R.F., 1974. Shear rate dependent viscosity of suspensions in Newtonian and non-Newtonian liquids. *Chemical Engineering Science*, 29(3), pp.729-735.
- [142] Novotny, E.J., 1977, January. Proppant transport. In SPE Annual Fall Technical Conference and Exhibition. Society of Petroleum Engineers.
- [143] Medvedev, A.V., Kraemer, C.C., Pena, A.A. and Panga, M.K.R., 2013, February. On the mechanisms of channel fracturing. In SPE Hydraulic Fracturing Technology Conference. Society of Petroleum Engineers.
- [144] McCaffery, S. J., Elliott, L., & Ingham, D. B., 1997 Enhanced Sedimentation In Inclined Fracture Channels, Topics in Engineering, (CD ROM ISBN 1-85312-546-6), 32.
- [145] Nott, P.R., Guazzelli, E. and Pouliquen, O., 2011. The suspension balance model revisited. *Physics of Fluids*, 23(4), p. 043304.
- [146] Oddie, G. and Pearson, J.A., 2004. Flow-rate measurement in two-phase flow. *Annu. Rev. Fluid Mech.*, 36, pp.149-172.
- [147] Asmolov, E.S., Osipov, A.A. 2008 Asymptotic Model of the Inertial Migration of Particles in a Dilute Suspension Flow Through the Entry Region of a Channel. *Phys. Fluids* 20 (12), 123301.
- [148] Osipov, A.A., Medvedev, O.O. and Willberg, D., Schlumberger Technology Corporation, 2008. Hydraulic fracture height growth control. U.S. Patent Application 12/998,866.
- [149] Nevkii, Yu. A., Osipov, A. N. 2009 Modeling gravitational convection in suspensions, *Technical Physics Letters*, 35, Issue 4, 340-343.
- [150] Nevkii, Yu. A., Osipov, A. N. 2011 Slow gravitational convection of disperse systems in domains with inclined boundaries, *Fluid Dynamics*, 46, Issue 2, 225-239.
- [151] Osipov, A.A., Sinkov, K.F. and Spesivtsev, P.E., 2014. Justification of the drift-flux model for two-phase flow in a circular pipe. *Fluid Dynamics*, 49(5), pp.614-626.
- [152] Krasnopolksky, B., Starostin, A. and Osipov, A.A., 2016. Unified graph-based multi-fluid model for gasliquid pipeline flows. *Computers & Mathematics with Applications*, 72(5), pp.1244-1262.
- [153] Osipov, A.A., Zilonova, E., Boronin, S., Desroches, J., Lebedeva, N. and Willberg, D., 2016, September. Insights on Overflushing Strategies from a Novel Modeling Approach to Displacement of Yield-Stress Fluids in a Fracture. In SPE Annual Technical Conference and Exhibition. Paper ID: SPE-181454-MS. Society of Petroleum Engineers.
- [154] Osipov, A.A. 2017 Hydraulic fracture conductivity: effects of rod-shaped proppant from lattice-Boltzmann simulations and lab tests. *Advances in Water Resources*, (Accepted, in Press). DOI: 10.1016/j.advwatres.2017.04.003
- [155] Osipov, A.A., Boronin, S., Zilonova, E., Desroches, J. 2017 Managed Saffman-Taylor Instability During Overflush in Hydraulic Fracturing, *Journal of Petroleum Science & Engineering*, (under review).
- [156] Ovarlez, G., Bertrand, F. and Rodts, S., 2006. Local determination of the constitutive law of a dense suspension of noncolloidal particles through magnetic resonance imaging. *Journal of Rheology*, 50(3), pp.259-292.
- [157] E. Ozkan, R. Raghavan, O.G. Apaydin, Modeling of Fluid Transfer from Shale Matrix to Fracture Network, SPE 134830, 2010. 18 pages.
- [158] Parlar, M., Nelson, E.B., Walton, I.C., Park, E. and DeBonis, V., 1995, January. An experimental study on fluid-loss behavior of fracturing fluids and formation damage in high-permeability porous media. In SPE Annual Technical Conference and Exhibition. Society of Petroleum Engineers.
- [159] Pearson, J.R., 1985. Mechanics of polymer processing. Springer Science

- & Business Media.
- [160] Pearson, J. R. A. 1994 On suspension transport in a fracture: framework for a global model. *J. Non-Newtonian Fluid Mech.* **54**, 503–513.
 - [161] Phillips, R.J., Armstrong, R.C., Brown, R.A., Graham, A.L. and Abbott, J.R., 1992. A constitutive equation for concentrated suspensions that accounts for shearinduced particle migration. *Physics of Fluids A: Fluid Dynamics* (1989-1993), 4(1), pp.30-40.
 - [162] Poiseuille, J., 1836. Observations of blood flow. *Ann Sci Nat STrie*, 5(2).
 - [163] Potapenko, D.I., Brown, J.E. and Lafferty, T., Schlumberger Technology Corporation, 2014. Well treatment. U.S. Patent Application 14/891,172.
 - [164] D.I. Potapenko, B.C. Theuveny, J. Desroches, D.M. Willberg, P. Enkababian, K. Moncada, R. Williams, P. Deslandes, N. Wilson, R. Neaton, M. Mikovich, Y. Han, G. Conort, Securing Long-Term Well Productivity of Horizontal Wells Through Optimization of Postfracturing Operations, SPE 187104 to be presented at the 2017 SPE Annual Technical Conference and Exhibition, San Antonio, TX, USA, 9-11 October 2017.
 - [165] Rajagopalan R., Tien C. Trajectory analysis of deepbed filtration with the sphere-in-cell porous media model, *AICHE Journal*, V. 22-3 pp. 523-533, 1976.
 - [166] Ray, B., Lewis, C., Martysevich, V., Shetty, D.A., Walters, H.G., Bai, J. and Ma, J., 2017, January. An Investigation into Proppant Dynamics in Hydraulic Fracturing. In SPE Hydraulic Fracturing Technology Conference and Exhibition. Society of Petroleum Engineers. SPE paper 184829-MS.
 - [167] Richardson, J.F. and Zaki, W.N., 1954. The sedimentation of a suspension of uniform spheres under conditions of viscous flow. *Chemical Engineering Science*, 3(2), 65-73.
 - [168] Romero, J., Mack, M.G. and Elbel, J.L., 1995, January. Theoretical model and numerical investigation of near-wellbore effects in hydraulic fracturing. In SPE annual technical conference and exhibition. Society of Petroleum Engineers.
 - [169] Roychaudhuri, B., Tsotsis, T.T. and Jessen, K., 2013. An experimental investigation of spontaneous imbibition in gas shales. *Journal of Petroleum Science and Engineering*, 111, pp.87-97.
 - [170] Bazilevskii, A.V., Koroteev, D.A., Rozhkov, A.N. and Skobeleva, A.A., 2010. Sedimentation of particles in shear flows of viscoelastic fluids. *Fluid Dynamics*, 45(4), pp.626-637.
 - [171] Bazilevsky, A.V., Kalinichenko, V.A., Plyashkevich, V.A., Badazhkov, D.V. and Rozhkov, A.N., 2016. Sedimentation of particles in shear flows of fluids with fibers. *Rheologica Acta*, 55(1), pp.11-22.
 - [172] R. Roscoe 1952 The viscosity of suspensions of rigid spheres, *Brit. J. Appl. Phys.* **3**, 267.
 - [173] Rubinow, S.I. and Keller, J.B., 1961. The transverse force on a spinning sphere moving in a viscous fluid. *Journal of Fluid Mechanics*, 11(03), pp.447-459.
 - [174] Saffman, P.G. and Taylor, G., 1958, June. The penetration of a fluid into a porous medium or Hele-Shaw cell containing a more viscous liquid. In Proceedings of the Royal Society of London A: Mathematical, Physical and Engineering Sciences, **245**, No. 1242, 312-329.
 - [175] Saffman, P.G.T., 1965. The lift on a small sphere in a slow shear flow. *Journal of fluid mechanics*, 22(02), pp.385-400. Saman P. G. 1968 Corrigendum. *J. Fluid Mech.* 31, 624.
 - [176] Schock, C.A. and Roco, M.C., 1991. *Slurry Flow*. Butterworth-Heinemann, Oxford.
 - [177] Scott, K.J., 1984. Hindered settling of a suspension of spheres: Critical evaluation of equations relating settling rate to mean particle diameter and suspension concentration. Council for Scientific and Industrial Research.
 - [178] Segre, G. and Silberberg, A., 1962. Behaviour of macroscopic rigid spheres in Poiseuille flow Part 2. Experimental results and interpretation. *Journal of Fluid Mechanics*, 14(01), pp.136-157.
 - [179] Settari, A., 1988, January. General model of fluid flow (leakoff) from fractures induced in injection operations. In SPE Annual Technical Conference and Exhibition. Society of Petroleum Engineers.
 - [180] Gadde, P.B., Liu, Y., Norman, J., Bonnecaze, R. and Sharma, M.M., 2004, January. Modeling proppant settling in water-fracs. In SPE annual technical conference and exhibition. Society of Petroleum Engineers.
 - [181] Malhotra, S. and Sharma, M.M., 2011, January. A General Correlation for Proppant Settling in VES Fluids. In SPE Hydraulic Fracturing Technology Conference. Society of Petroleum Engineers.
 - [182] Malhotra, S., Lehman, E.R. and Sharma, M.M., 2014. Proppant placement using alternate-slug fracturing. *SPE Journal*, 19(05), pp.974-985.
 - [183] Karantinos, E., Sharma, M.M., Ayoub, J.A., Parlar, M. and Chanpura, R.A., 2016, February. Choke Management Strategies for Hydraulically Fractured Wells and FracPack Completions in Vertical Wells. In SPE International Conference and Exhibition on Formation Damage Control. Society of Petroleum Engineers.
 - [184] Blyton, C. A. J., and Sharma, M. M. 2017 Particle transport of non-dilute suspensions in branched slots, *Int. J. of Multiphase Flow*, Submitted.
 - [185] Sahai, R., Miskimins, J. L., & Olson, K. E. 2014. Laboratory results of proppant transport in complex fracture systems. In SPE Hydraulic Fracturing Technology Conference. Society of Petroleum Engineers.
 - [186] Shi, H., Holmes, J.A., Durlofsky, L.J., Aziz, K., Diaz, L., Alkaya, B. and Oddie, G., 2005. Drift-flux modeling of two-phase flow in wellbores. *Spe Journal*, 10(01), pp.24-33.
 - [187] Shi, H., Holmes, J., Diaz, L., Durlofsky, L.J. and Aziz, K., 2005. Drift-flux parameters for three-phase steady-state flow in wellbores. *SPE Journal*, 10(02), pp.130-137.
 - [188] McClure, M., Babazadeh, M., Shiozawa, S. and Huang, J., 2015, February. Fully coupled hydromechanical simulation of hydraulic fracturing in three-dimensional discrete fracture networks. In SPE Hydraulic Fracturing Technology Conference. Society of Petroleum Engineers.
 - [189] Shiozawa, S. and McClure, M., 2016. Simulation of proppant transport with gravitational settling and fracture closure in a three-dimensional hydraulic fracturing simulator. *Journal of Petroleum Science and Engineering*, 138, pp.298-314.
 - [190] Siebrits, E., Gu, H. and Desroches, J., 2001. An improved pseudo-3D hydraulic fracturing simulator for multiple layered materials. *Computer Methods and Advances in Geomechanics*, pp.1341-1345.
 - [191] Siebrits, E. and Peirce, A.P., 2002. An efficient multilayer planar 3D fracture growth algorithm using a fixed mesh approach. *International Journal for Numerical Methods in Engineering*, 53(3), pp.691-717.
 - [192] Sinkov K. F., Spesivtsev P. E., Osipov A.A. 2014. Simulation of particles transport in multiphase pipe flow for cleanup of oil and gas wells, 19th International Conference on Hydrotransport. BHR Group. Golden, Colorado, USA: 2014. September 24-26. pp. 516.
 - [193] Snook, B., Davidson, L.M., Butler, J.E., Pouliquen, O. and Guazzelli, E., 2014. Normal stress differences in suspensions of rigid fibres. *Journal of Fluid Mechanics*, 758, pp.486-507.
 - [194] Smirnov, N.N., Nikitin, V.F., Maximenko, A., Thiercelin, M. and Legros, J.C., 2005. Instability and mixing flux in frontal displacement of viscous fluids from porous media. *Physics of fluids*, 17(8), p.084102.
 - [195] Thomas, D.G., 1965. Transport characteristics of suspension: VIII. A note on the viscosity of Newtonian suspensions of uniform spherical particles. *Journal of Colloid Science*, 20(3), 267-277.
 - [196] Kharlashkin, A. 2017. Mathematical Modeling of Multiphase Flows in Long Pipelines, MSc Thesis, Faculty of Mechanics and Mathematics, Lomonosov Moscow State University.
 - [197] Soopyan, F.B., Cremaschi, S., Sarica, C., Subramani, H.J. and Kouba, G.E., 2014. Solids transport models comparison and finetuning for horizontal, low concentration flow in singlephase carrier fluid. *AICHE Journal*, 60(1), pp.76-122.
 - [198] Stickel, J.J. and Powell, R.L., 2005 Fluid mechanics and rheology of dense suspensions. *Annu. Rev. Fluid Mech.*, **37**, 129-149.
 - [199] Suarez-Rivera, R., Behrmann, L.A., Green, S., Burghardt, J., Stanchits, S., Edelman, E. and Surdi, A., 2013, September. Defining three regions of hydraulic fracture connectivity, in unconventional reservoirs, help designing completions with improved long-term productivity. In SPE Annual Technical Conference and Exhibition. Society of Petroleum Engineers.
 - [200] Starostin, A.B., Krasnopol'sky, B.I. and Lukyanov, A.A., 2016, August. Phase Switching Algorithm for Slug Flows in Wellbores. In *ECMOR XV-15th European Conference on the Mathematics of Oil Recovery*.
 - [201] Tang, H., Winterfeld, P.H., Wu, Y.S., Huang, Z.Q., Di, Y., Pan, Z. and Zhang, J., 2016. Integrated simulation of multi-stage hydraulic fracturing in unconventional reservoirs. *Journal of Natural Gas Science and Engineering*, 36, pp.875-892.
 - [202] Taylor, G.I. 1954 The dispersion of matter in turbulent flow through a pipe. *Pr. R. Soc. London. Ser. A.* **223** (1155), 446-468.
 - [203] Tehrani, M.A., 1996 An experimental study of particle migration in pipe flow of viscoelastic fluids. *Journal of Rheology*, 40(6), 1057-1077.
 - [204] Theuveny, B.C., Mikhailov, D., Spesivtsev, P., Starostin, A., Osipov, A.A., Sidorova, M. and Shako, V., 2013, September. Integrated approach to simulation of near-wellbore and wellbore cleanup. In SPE Annual

- Technical Conference and Exhibition. Society of Petroleum Engineers.
- [205] Torquato, S., Truskett, T.M. and Debenedetti, P.G., 2000. Is random close packing of spheres well defined?. *Physical review letters*, 84(10), p.2064.
- [206] Unwin, A.T. and Hammond, P.S., 1995, January. Computer simulations of proppant transport in a hydraulic fracture. In SPE Western Regional Meeting. Society of Petroleum Engineers.
- [207] Vasudevan, S., Willberg, D.M., Wise, J.A., Gorham, T.L., Dacar, R.C., Sullivan, P.F., Boney, C.L. and Mueller, F., 2001, January. Field Test of a Novel Low Viscosity Fracturing Fluid in the Lost Hills Field, California. In SPE Western Regional Meeting. Society of Petroleum Engineers.
- [208] S. Vasudevan, P. Sullivan, J. Desroches and D. Willberg, "Development of a New Bridging Criterion for Hydraulic Fracturing", Proceedings of the 6th World Congress of Chemical Engineering. Melbourne, Australia. 23-27 September 2001. pp. 1-11.
- [209] Weng, X., Kresse, O., Chuprakov, D., Cohen, C.E., Prioul, R. and Ganguly, U., 2014. Applying complex fracture model and integrated workflow in unconventional reservoirs. *Journal of Petroleum Science and Engineering*, 124, pp.468-483.
- [210] Van Dam, D. B., & de Pater, C. J. 1999. Roughness of hydraulic fractures: the importance of in-situ stress and tip processes. In SPE Annual Technical Conference and Exhibition. Society of Petroleum Engineers.
- [211] Van der Vlis, A.C., Haafkens, R., Schipper, B.A. and Visser, W., 1975, January. Criteria for proppant placement and fracture conductivity. In Fall Meeting of the Society of Petroleum Engineers of AIME. Society of Petroleum Engineers.
- [212] Vasseur, P. and Cox, R.G., 1976. The lateral migration of a spherical particle in two-dimensional shear flows. *Journal of Fluid Mechanics*, 78(02), pp.385-413.
- [213] Walton, I. C. 1991 Eddy diffusivity of solid particles in a turbulent liquid flow in a horizontal pipe, *AIChE*, 41(7), 1815-1820.
- [214] Walton, I. and McLennan, J., 2013, May. The role of natural fractures in shale gas production. In ISRM International Conference for Effective and Sustainable Hydraulic Fracturing. International Society for Rock Mechanics.
- [215] Wang, J. S. Y., T. N. Narasimhan, and C. H. Scholz. 1988. Aperture correlation of a fractal fracture. *Journal of Geophysical Research: Solid Earth*, 93 (B3), 2216-2224.
- [216] Willberg, D.M., Steinsberger, N., Hoover, R., Card, R.J. and Queen, J., 1998, January. Optimization of Fracture Cleanup Using Flowback Analysis. In SPE Rocky Mountain Regional/Low-Permeability Reservoirs Symposium. Society of Petroleum Engineers. pp. 147-159. SPE paper 39920-MS.
- [217] Williams, B.B., 1970. Fluid loss from hydraulically induced fractures. *Journal of Petroleum Technology*, 22(07), pp.882-888.
- [218] Xu, W., Thiercelin, M.J., Ganguly, U., Weng, X., Gu, H., Onda, H., Sun, J. and Le Calvez, J., 2010, January. Wiremesh: a novel shale fracturing simulator. In International Oil and Gas Conference and Exhibition in China. Society of Petroleum Engineers
- [219] Xu, W., 2014, August. Modeling Gas Transport in Shale Reservoir-Conservation Laws Revisited. In SPE/AAPG/SEG Unconventional Resources Technology Conference. Society of Petroleum Engineers.
- [220] Zhang, G., Gutierrez, M. and Li, M., 2017. A coupled CFD-DEM approach to model particle-fluid mixture transport between two parallel plates to improve understanding of proppant micromechanics in hydraulic fractures. *Powder Technology*, 308, pp.235-248.
- [221] Zhang, G., Gutierrez, M. and Li, M., 2017. Numerical simulation of transport and placement of multi-sized proppants in a hydraulic fracture in vertical wells. *Granular Matter*, 19(2), p.32.
- [222] V.Zhibaedov, N.Lebedeva, K.Sinkov, and A.Osiptsov, 2016. On hyperbolicity of 1D models for transient two-phase flows in pipelines, *Fluid Dynamics*. V. 51. N1. pp. 51-69.
- [223] Zamani A., Maini B. Flow of dispersed particles through porous media-deep bed filtration, *Journal of Petroleum Science and Engineering*, V. 691, pp. 71-88, 2009.

Symbol	Definition
a	Particle radius
α	Exponent in hindered-settling correction factor
β	Exponent in expression for slurry viscosity
b	Bridging factor
Bn	Bingham number
Bu	Buoyancy number
C_D	Drag coefficient of a sphere
C_L	Leak-off coefficient
C_{max}	Maximum packing concentration of particles
C_p	Particle volume concentration
δ	Characteristic size of the fracture face roughness
d	Particle diameter
D	Pipe diameter
De	Deborah number
e	Rate-of-strain tensor
ε	Small width-to-length fracture aspect ratio
ε_p	Particle diffusivity
F	Force
Fr	Froude number
f_{se}	Slurry friction factor
ϕ	Porosity
Φ	Coefficient with fluid mobility due to yield stress
$\dot{\gamma}$	Shear rate
ϑ	Term due to yield stress in fluid mobility coeff.
h, H	Height
I	Non-dimensional viscous number in frictional rheology
K	Consistency of the fluid
Kn	Knudsen number
K_b	Klinkenberg constant
K_p	Permeability of the proppant pack
K_c, K_μ	Coefficients in diffusive-flux model
λ	Molecular diffusivity
μ	Dynamic viscosity
N_1, N_2	Normal stresses
n	Behavior index in the power-law rheology model
p, p_{ij}	Pressure, stress tensor
R	Height-to-length aspect ratio of the fracture
Re	Channel Reynolds number
Re_p	Particle Reynolds number
σ	Mean free path between interparticle collisions
σ_n	Closure stress
St	Stokes number
τ	Shear stress
T	Granular temperature of suspension
T_L	Fluid Lagrangian time scale
t_0	Time of the start of leak-off in Carter's model
t_r	Relaxation time of the medium
t_s	Particle relaxation time
v_L	Leak-off velocity
U	Linear velocity
\mathbf{v}	Velocity vector (general)
w	Fracture width
We	Weissenberg number
ζ	Density ratio
M	Viscosity ratio

Table 9: Nomenclature: symbols and their definitions.

- Review of fundamental issues in fluid mechanics of hydraulic fracturing / flowback.
- Application is hydraulic fracture simulation software used to design treatments.
- Research structure: 1D transport in wells, 2D flow in fracs & multiscale flowback.
- Closures from lab for particle settling, suspension rheology, etc. are paramount.
- Review is designed as a white paper: state-of-art, key issues and way forward.